Archival Report

Biological Psychiatry

Divergent Modulation of Dopaminergic Neurons by Hypocretin/Orexin Receptors 1 and 2 Shapes Dopaminergic Cell Activity and Socioemotional Behavior

Stamatina Tzanoulinou, Simone Astori, Laura Clara Grandi, Francesca Gullo, Richie Kalusivikako, Simran Rai, Galina Limorenko, Mehdi Tafti, Andrea Becchetti, and Anne Vassalli

ABSTRACT

BACKGROUND: Many neuropsychiatric disorders involve dysregulation of the dopaminergic (DA) input to the forebrain. DA afferents from the midbrain ventral tegmental area (VTA) are particularly relevant. A key neuromodulatory influence on DA^{VTA} neurons arises from lateral hypothalamic area hypocretin/orexin (OX) neurons. Despite being a major input, the differential actions of OX peptides A and B on their receptors (OX_1R and OX_2R) in DA neurons are poorly understood.

METHODS: Using genetically engineered mice whose DA cells selectively lack OX input via *Hcrtr1* ($DA^{Ox1R\text{-}KO}$) or *Hcrtr2* ($DA^{Ox2R\text{-}KO}$), we assessed DA^{VTA} neuron intrinsic excitability ex vivo and evaluated behavioral phenotypes across socioemotional and cognitive domains.

RESULTS: We discovered previously unrecognized effects of OX peptides on DA^{VTA} cell response. While OXA enhanced DA^{VTA} neuron firing via OX_1Rs, OXB diminished firing via OX_2Rs. Behaviorally, DA OX_1R loss generated anxiety-like responding and context-dependent hyperactivity, while DA OX_2R loss decreased sociability and compromised aversion-driven learning. Loss of either OX_1Rs or OX_2Rs in DA cells elicited impulsivity and compulsivity-like behavioral patterns.

CONCLUSIONS: We evidenced distinct functions of OX_1R versus OX_2R signaling in modulating the intrinsic excitability of DA^{VTA} neurons and influencing DA-related behaviors. Our data implicate OX→DA signaling pathways in neuropsychiatric endophenotypes relevant to obsessive-compulsive, attention-deficit/hyperactivity, and autism spectrum disorders and inform therapeutic strategies targeting OX receptors.

https://doi.org/10.1016/j.biopsych.2026.05.022

By altering neuronal excitability and synaptic efficacy, neuromodulators reconfigure neural circuits and drive brain state shifts, often acting via volume transmission and engaging both synaptic and extrasynaptic receptors. Among them, dopamine (DA) and hypocretin/orexin (OX) are 2 key modulators of arousal and motivation (1) whose interplay remains underexplored.

Orexin peptides A and B are exclusively produced by a small set of lateral hypothalamic area (LHA) glutamatergic neurons that send brainwide projections and signal via 2 G protein-coupled receptors: *Hcrtr1* gene-encoded OX_1R and *Hcrtr2*-encoded OX_2R. Orexin A (OXA) is reported to bind both receptors with high affinity, whereas orexin B (OXB) has high affinity only for OX_2Rs (2,3).

OX cells fire maximally during active wakefulness, but they also fire transiently during non–rapid eye movement (REM) sleep (4) and phasic REM sleep (5) and are key sleep/wake state regulators. Accordingly, OX deficiency severely compromises the integrity, stability, and sequence of vigilance states (6,7), causing narcolepsy type 1 (8).

Although dog and mouse genetics point to stronger OX_2R involvement in state regulation, many studies focused on OXA/OX_1R, leaving OX_1R versus OX_2R differential functions underexplored, despite their suspected involvement in neuropsychiatric disorders (9).

Beyond sleep/wake control, OXs are central for energy homeostasis, reward, autonomic, endocrine functions, and mood-related behaviors (10,11). OX neurons innervate all wake-promoting monoaminergic and cholinergic nuclei and their targets in the neocortex, thalamus, forebrain, and spinal cord, specifically the basal forebrain, locus coeruleus, dorsal raphe, extended amygdala, ventral tegmental area (VTA), nucleus accumbens (NAc), and medial prefrontal cortex (mPFC) (12–14). Among OX targets, DA stands out as a major OX effector. Narcolepsy type 1's hallmark symptoms—daytime sleepiness and cataplexy—both result from OX deficiency,

SEE COMMENTARY ON PAGE 722

ISSN: 0006-3223

but while engaging distinct mechanisms (15), both respond to dopaminergic drugs (16,17). OX neurons densely innervate DA^{VTA} neurons, which express both *Hcrtr1* and *Hcrtr2* (18), positioning the $OX^{LHA} \rightarrow DA^{VTA}$ circuit as a critical component of OX-DA interactions (11,19–25). Electron microscopy studies have revealed that many VTA OX axons are en-passant fibers, with numerous dense-cored vesicles suggesting nonsynaptic effects (26).

DA^{VTA} subpopulations exhibited varied responses to OXs. OXA elevated $[Ca^{2+}]_{cytosolic}$ in isolated DA^{VTA} cells (27) and enhanced firing in slices, while OXB enhanced firing in some cells but elicited alternate periods of hyperpolarization and firing in others (28).

OXA is thought to stimulate DA^{VTA} activity both by direct somatodendritic OXR activation and indirect glutamatergic afferent potentiation (28–30). OXA potentiates DA^{VTA} cell NMDA receptor transmission, while intra-VTA OX_1R antagonism blocked mouse locomotor sensitization to cocaine and ex vivo DA^{VTA} AMPA/NMDA ratio increase, a proxy for plasticity, normally observed after cocaine exposure (29). Optical stimulation of VTA OX terminals did not increase NAc DA release but did so when paired with intra-VTA electrical stimulation (31), suggesting that OXA/OX_1R signaling potentiates $DA^{VTA} \rightarrow$ NAc transmission by recruiting glutamatergic afferents.

To cell autonomously interrogate OX effects in DA cells, we selectively inactivated the *Hcrtr1* or *Hcrtr2* gene in DA cells. DA-specific *Ox2R* loss led to electrocortical hyperarousal and improved reward-based learning and attention but caused impulsive and compulsive-like behaviors (18). Here, we systematically investigated the electrophysiological correlates of deleting *Hcrtr1*/*Ox1R* versus *Hcrtr2*/*Ox2R* in DA^{VTA} cells and further evaluated behavioral effects. We revealed strikingly distinct functions of OX_1Rs versus OX_2Rs and uncovered an unsuspected OX_2R-mediated DA^{VTA} cell inhibition, thereby raising important questions for OXR-targeted therapeutics development.

METHODS AND MATERIALS

Animals

All procedures followed Swiss National Institutional Guidelines on Animal Experimentation, approved by Cantonal Veterinary Office Committee, except dissociated DA^{VTA} cell ex vivo recordings, which were performed in Italy, following Italian laws, approved by the Italian Ministry of Health and local Ethical Committee.

Patch-Clamp Recording of Dissociated DA^{VTA} Neurons

Cells were dissociated from acute brain slices of postnatal day 13 to postnatal day 18 wild-type C57BL/6J or $Hcrtr2^{\Delta/\Delta}$ mice (Figure 1). DA cells were identified by slow spontaneous firing and rapid firing blockade by 100 μM DA (32). Patch-clamp recordings were performed in cell-attached or perforated-patch configuration.

Patch-Clamp Recording of DA^{VTA} Neurons in Slices

To examine the impact of selective *Ox1R* or *Ox2R* knockout (KO), we performed patch-clamp recordings of DA^{VTA} neurons in slices from $DA^{Ox1R\text{-}KO}$ and $DA^{Ox2R\text{-}KO}$ mice and controls, targeting the lateral VTA (Figure 2A), reported to contain OX-responding NAc-projecting DA cells (33). To isolate intrinsic excitability in response to OXs, we stimulated DA^{VTA} cells to fire at regular intervals by applying depolarizing current injections.

Behavior

After showing that OXA and OXB peptides exert opposite actions on DA^{VTA} cell intrinsic excitability and that their impact is lost in $DA^{Ox1R\text{-}KO}$ and $DA^{Ox2R\text{-}KO}$ mice, respectively, we sought to determine the behavioral correlates of the 2 divergent $OX \rightarrow DA$ pathways by exposing mice to a panel of tests. We selected paradigms representing 4 axes heavily dependent on OX and DA transmission (Figure S2): positive affect (rewarding: sociability) and negative affect (aversive: active avoidance)–related, anxiety-like (open field, elevated plus maze [EPM]), and cognitive (3-choice serial reaction time task [3-CSRTT]) behaviors. All tests were performed in the light phase after ensuring similar results in light and dark phases (Figure S3).

Further description of the Methods and Materials is provided in the Supplement.

RESULTS

Opposite Effects of OXA Versus OXB on Dissociated DA^{VTA} Neurons

OXA was reported to increase firing of DA neurons in rat VTA slices, whereas OXB could induce phasic firing (28). To assess cell-autonomous modulation by OXs, we performed patch-clamp recordings of dissociated DA cells from wild-type VTA slices. Spontaneous action currents were recorded in cell-attached mode in 1-minute bins before, during, and after OX application (34). OXA (100 nM) increased DA^{VTA} spontaneous activity in 80% of tested cells, consistent with previous data in slices (28,33), with a slow recovery (Figure 1A, Ci). In contrast, within 1 to 2 minutes of exposure, OXB (100 nM) decreased DA^{VTA} cell firing frequency by 20% to 25% in 70% of cells, with relatively rapid recovery upon peptide removal (Figure 1Cii). Stronger firing decrease (~40%) was elicited by the OX_2R-selective agonist [Ala^{11},D-Leu^{15}]-OXB (OXB-AL) (35) (200 nM) (Figure 1B top, Ciii). To complement cell-attached measurements, OXB-AL was also tested in perforated-patch condition, with similar results (Figure 1B, bottom). Given OXB's high OX_2R affinity but poor OX_1R binding, we tested DA^{VTA} cells from $Hcrtr2^{\Delta/\Delta}$ mice, which lack the *Hcrtr2* gene, and thus OX_2Rs, in all cells (18). OXB (100 nM) only exerted minor effects on DA^{VTA} cells from $Hcrtr2^{\Delta/\Delta}$ mice (Figure 1Cii), validating the predominantly OX_2R-dependent effect of OXB. To substantiate these results, we measured DA^{VTA} response to a nonpeptidic OX_2R agonist, YNT-185 (Figure 1D). Consistent with OXB and OXB-AL, YNT-185 (2 μM) inhibited DA^{VTA} cell firing by 30% on average. The YNT-185 concentration-response curve resembled that of *Ox2R*-transfected cell (36) (Figure 1Di), with half maximal effective concentration ≈ 250 nM, about one order of magnitude lower than for *Ox1R*. At 5 μM, YNT-185 inhibitory effects

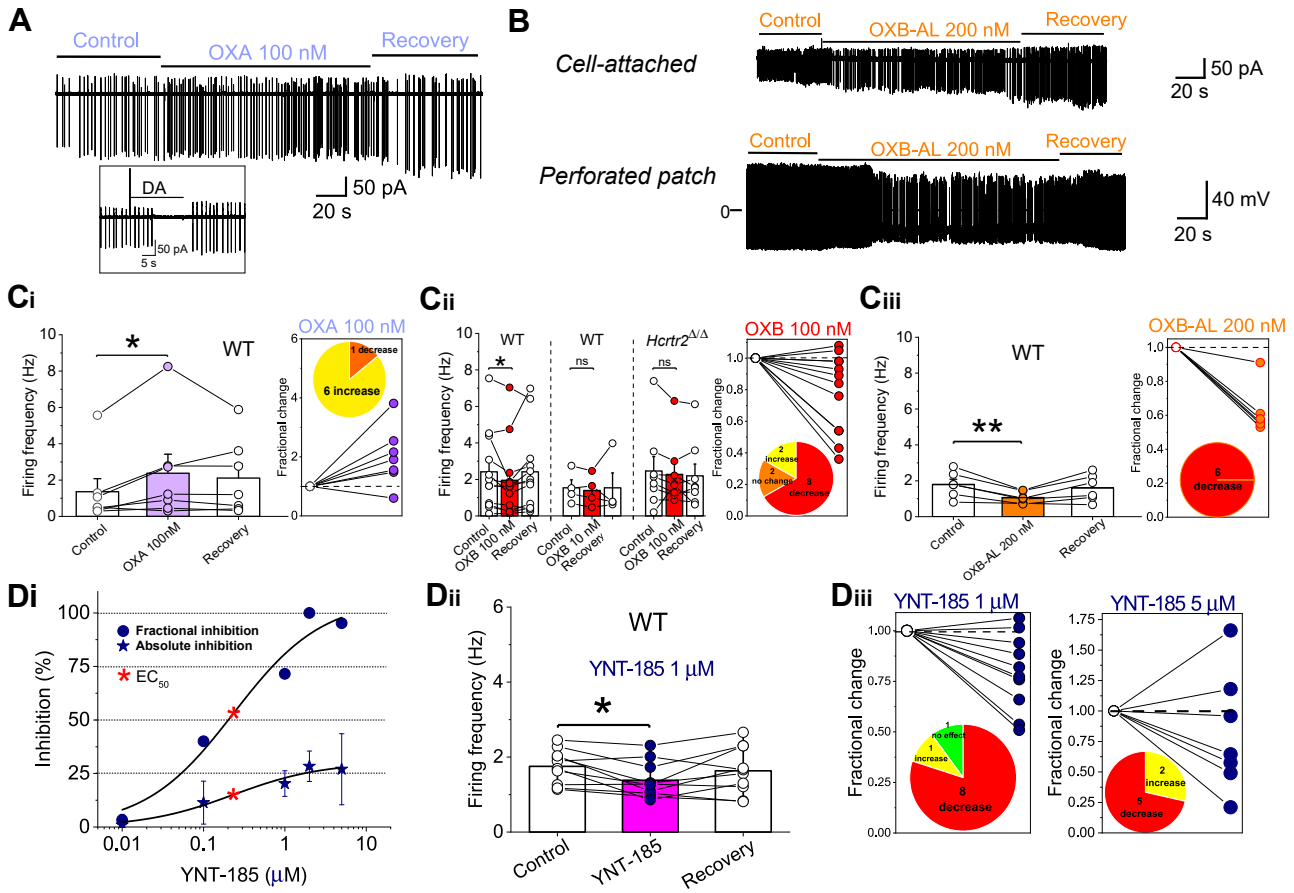

Figure 1. OXA increases while OXB and OX_2R-specific agonists decrease firing of dissociated DA^{VTA} cells from WT mice. DA cells were acutely isolated from VTA slices of C57BL/6J (WT) or *Hcrtr2*$^{\Delta/\Delta}$ (OX_2R-deficient) (18) mice at 2 to 3 weeks of age. Spontaneous firing activity was assessed by recording action currents in cell-attached mode **(A–D)** or action potentials in perforated patch mode **(B)**, before (control), during, and after (recovery) bath application of OXA (100 nM), OXB (10 or 100 nM), or the OX_2R-specific agonists OXB-AL (200 nM) or YNT-185 (10 nM–5 μM). **(A)** Representative trace showing spontaneous firing of a WT DA cell exposed first to DA (inset) and next to OXA. **(B)** (Top) Representative trace showing spontaneous firing of a WT DA cell exposed to OXB-AL. (Bottom) Voltage trace showing spontaneous firing recorded through perforated patch of a WT DA cell exposed to OXB-AL, before (control), during (OXB-AL 200 nM), and after (recovery) application of the peptide (representative of 3 experiments). **(Ci)** Firing frequencies calculated before (control; 2 minutes), during the second minute of OXA exposure (purple), or after washout (recovery). Bar graphs: control: 1.36 ± 0.717 Hz; OXA: 2.374 ± 1.05 Hz; recovery: 2.11 ± 0.79 Hz (χ^2_2 = 6, p = .0498; Friedman ANOVA; post hoc Wilcoxon-Nemenyi-McDonald-Thompson test between control and OXA: p = .043, n = 7). (Inset) Relative effect of OXA on firing activity in individual WT DA cells. Each data point (purple) is the OXA firing frequency of an individual cell, normalized to its control value (white). Pie chart: number of cells responding positively (yellow) or negatively (red) to OXA. **(Cii)** Firing frequencies calculated before (control; 2 minutes), during the first minute of OXB exposure (red), or after washout (recovery). Left bar graphs (WT): control: 2.42 ± 0.63 Hz; OXB 100 nM: 1.955 ± 0.59 Hz (χ^2_2 = 8.17, p = .01685; Friedman ANOVA; post hoc WNMT test between control and OXB: p = .022; n = 12); recovery: 2.42 ± 0.64 Hz. Middle bar graphs (WT): control: 1.54 ± 0.44 Hz; OXB 10 nM: 1.39 ± 0.43 Hz (F = 0.09834, p = .78, repeated-measures 1-way ANOVA; n = 4); recovery: 1.54 ± 0.81 Hz. Right bar graphs (*Hcrtr2*$^{\Delta/\Delta}$) depict data recorded from DA neurons isolated from VTA slices from *Hcrtr2*$^{\Delta/\Delta}$ mice: control 2.46 ± 0.79 Hz; OXB 100 nM: 2.28 ± 0.62 Hz (χ^2_2 = 3.25, p = .197; Friedman ANOVA; n = 8); recovery: 2.195 ± 0.65 Hz. (Inset) Relative effect of OXB 100 nM (red) on firing activity in individual WT DA cells, calculated as in **(Ci)**. Pie chart: number of cells responding positively (yellow), negatively (red), or not responding (green; <2% absolute response) to OXB 100 nM. **(Ciii)** (Right) Firing frequencies calculated before (control, 2 minutes), during the first minute of OXB-AL exposure (orange), or after washout (recovery). Bar graphs: control: 1.8 ± 0.293 Hz; OXB-AL: 1.06 ± 0.137 Hz (F = 12.16, p = .002; repeated-measures 1-way ANOVA; post hoc Holm-Sidak test between control and OXB-AL: p = .0008, n = 6); recovery: 1.61 ± 0.31 Hz. (Inset) Relative effect of OXB-AL (orange) on firing activity in individual WT DA cells, calculated as in **(Ci)**. Pie chart: All cells responded negatively to OXB-AL. **(Di)** Different concentrations of YNT-185 were tested on WT DA cell spontaneous firing frequency, as in **(A–C)**. Stars: average percentage inhibitory effect of the indicated agonist concentrations. Circles: average inhibitory effect normalized to the maximal effect (at 2 μM); continuous lines are Hill-type functions best fitting the experimental data points (half-effective inhibitory concentration: 0.23 ± 0.22 μM; n_{Hill} = 0.79 ± 0.398). **(Dii)** Detailed statistics for 1 μM YNT-185 (control: 1.75 ± 0.145 Hz; YNT-185: 1.382 ± 0.152 Hz; F = 4.86, p = 2.4 × 10^{-6}; repeated-measures 1-way ANOVA; post hoc Holm-Sidak test between control and OXB-AL: p = .007, n = 10); recovery: 1.633 ± 0.199 Hz. **(Diii)** (Left) Relative effect of YNT-185 1 μM (navy) on firing activity in individual WT DA cells, calculated as in **(Ci)**. Pie chart: number of cells responding positively (yellow), negatively (red), or not responding (green; <2% absolute response) to the agonist. (Right) Same as left panel for YNT-185 5 μM. *p < .05, **p < .01. ANOVA, analysis of variance; DA, dopamine; EC_{50}, half maximal effective concentration; ns, nonsignificant; OXA, orexin A; OXB, orexin B; VTA, ventral tegmental area; WT, wild-type.

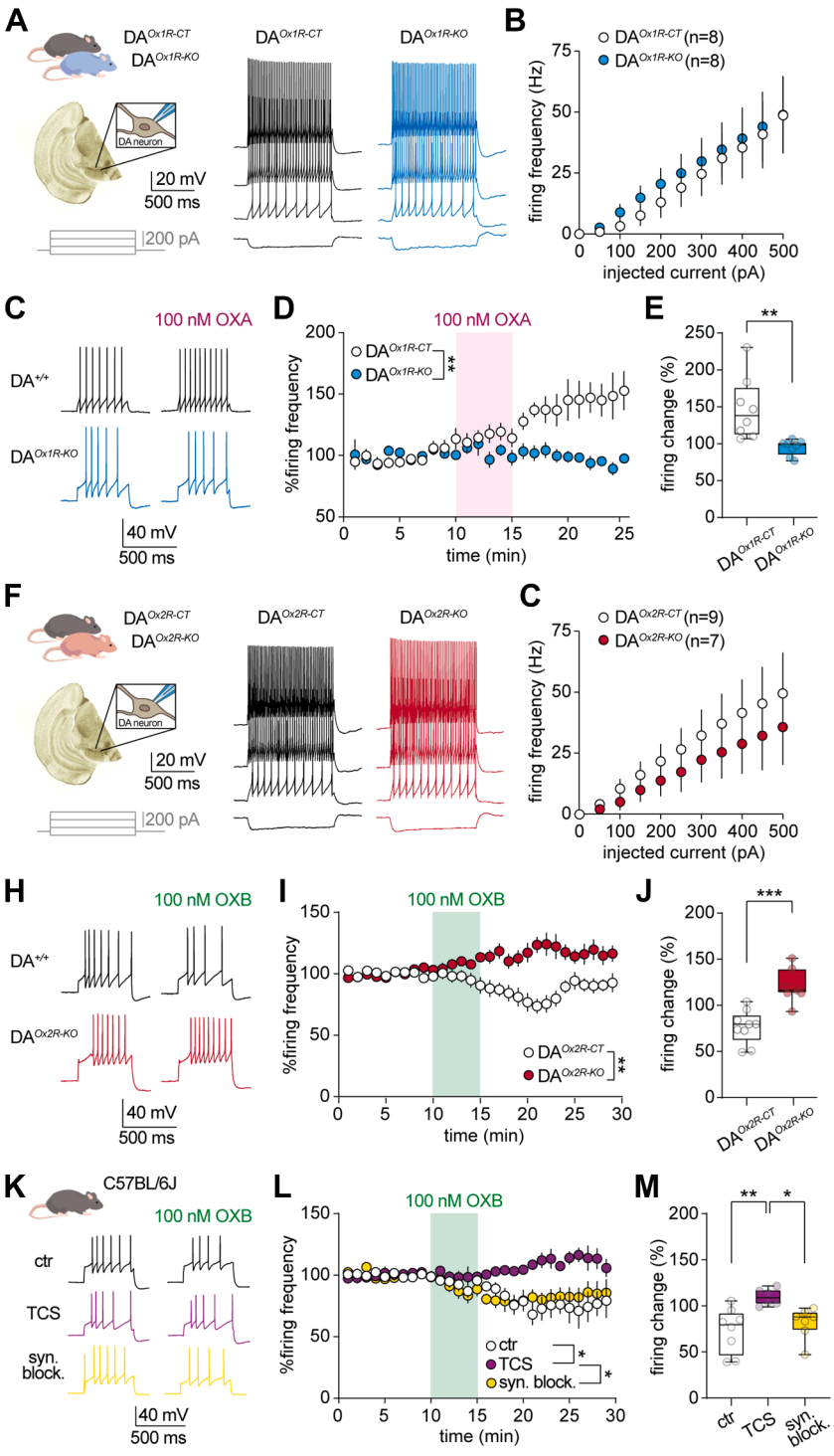

Figure 2. Orexin peptides bidirectionally modulate the excitability of DA^{VTA} neurons via OX_1R and OX_2R signaling. **(A)** Scheme of whole-cell patch-clamp recordings from DA neurons in VTA slices from $DA^{Ox1R\text{-}CT}$ and $DA^{Ox1R\text{-}KO}$ mice and representative traces of neuronal firing elicited by increasing somatic current injections. **(B)** Frequency-current relationship of action potential discharges shows no difference between genotypes (2-way ANOVA for effect genotype $F_{1,14}$ = 0.1426, p = .711). **(C)** Examples of neuronal firing in response to a depolarizing step prior to and after bath application of OXA (100 nM) in DA^{VTA} cells from $DA^{Ox1R\text{-}CT}$ and $DA^{Ox1R\text{-}KO}$ mice. **(D)** Mean firing frequency values normalized to the first 10 minutes (n = 8 cells per genotype). OXA increased firing in $DA^{Ox1R\text{-}CT}$ but not $DA^{Ox1R\text{-}KO}$ mice (2-way ANOVA for effect genotype $F_{1,14}$ = 10.45, p = .006 and genotype × treatment interaction $F_{24,334}$ = 5.772, $p < .001$). **(E)** Average OXA-induced change in neuronal firing in $DA^{Ox1R\text{-}CT}$ and $DA^{Ox1R\text{-}KO}$ mice ($t_{7.87}$ = 3.419, p = .009, t test). **(F)** Experimental scheme and examples of firing in DA^{VTA} neurons from $DA^{Ox2R\text{-}CT}$ and $DA^{Ox2R\text{-}KO}$ mice. **(G)** Frequency-current relationship of action potential discharges shows no difference between genotypes (2-way ANOVA for effect genotype $F_{1,14}$ = 0.457, p = .510). **(H)** Examples of neuronal firing prior to and after bath application of OXB (100 nM) in DA^{VTA} cells from $DA^{Ox2R\text{-}CT}$ and $DA^{Ox2R\text{-}KO}$ mice. **(I)** Mean firing frequency values normalized to the first 10 minutes (n = 9:7 cells, CT:KO). OXB transiently decreased firing in $DA^{Ox2R\text{-}CT}$ (paired t test; t_8 = 3.546, p = .008) but not $DA^{Ox2R\text{-}KO}$ mice, which instead showed a tendency toward increased firing (t_6 = 2.132, p = .077, paired t test). Two-way ANOVA revealed a genotype effect ($F_{1,14}$ = 14.87, p = .002) and a significant genotype × treatment interaction ($F_{28,383}$ = 6.484, $p < .001$). **(J)** Average OXB-induced change in neuronal firing in $DA^{Ox2R\text{-}CT}$ and $DA^{Ox2R\text{-}KO}$ mice ($t_{12.72}$ = 4.729, $p < .001$, t test). **(K)** Examples of neuronal firing before and after bath application of OXB (100 nM) in DA^{VTA} neurons from C57BL/6J mice under 3 conditions: control (without blockers), in the presence of the OX_2R antagonist TCS-OX2-29 (10 μM), and in the presence of synaptic blockers (10 μM DNQX, 50 μM D,L-APV, 100 μM picrotoxin). **(L)** Mean firing frequency normalized to the first 10 minutes for each experimental group (n = 8, 6, 7, respectively). OXB decreased firing in the ctr condition (W = −32, p = .023, Wilcoxon test) and in the presence of synaptic blockers (t_6 = 2.634, p = .039, paired t test), but not when OX_2R receptors were blocked (t_6 = 1.662, p = .148, paired t test). A mixed-effects analysis revealed a significant effect of OXB ($F_{30,570}$ = 2.787, $p < .001$) and a significant effect of the blockers ($F_{2,18}$ = 6.433, $p < .01$). **(M)** Average OXB-induced change in neuronal firing across the 3 groups ($F_{2,18}$ = 6.815, p = .006, 1-way ANOVA, followed by Holm-Šídák's multiple comparisons test). Bar graphs show individual values and mean ± SEM. Timelines show mean ± SEM. $^*p < .05$, $^{**}p < .01$, $^{***}p < .001$. ANOVA, analysis of variance; CT, control genotype mouse group; ctr, control; DA, dopamine; KO, knockout genotype mouse group; OXA, orexin A; OXB, orexin B; syn. bloc., synaptic blockers; VTA, ventral tegmental area.

were less pronounced, and data points were more scattered (Figure 1Dii, Diii), which we attribute to partial engagement of OX_1Rs at concentrations >2–3 μM (36).

These findings confirm that OXA increases DA^{VTA} neuronal firing and reveal that OXB-mediated OX_2R signaling can decrease DA^{VTA} neuronal firing, underscoring previously

unrecognized differences between OX_1R and OX_2R dopaminergic transduction.

Opposite Effects of OX_1R Versus OX_2R Activation on DA^{VTA} Cell Firing in Slices

To corroborate the results from dissociated cells and examine the impact of selective *Ox1R*- or *Ox2R*-KO, we performed patch-clamp recordings of DA^{VTA} neurons in slices from $DA^{Ox1R\text{-}KO}$ and $DA^{Ox2R\text{-}KO}$ mice and respective controls ($DA^{Ox1R\text{-}CT}$ and $DA^{Ox2R\text{-}CT}$). We examined intrinsic excitability of DA^{VTA} cells through patch-clamp recordings in the lateral VTA (Figure 2A).

Depolarizing current injections (Figure 2A, B) revealed no $DA^{Ox1R\text{-}KO}$ versus $DA^{Ox1R\text{-}CT}$ genotype differences in firing frequency-current relationships, indicating that *Ox1R*-KO does not alter basal DA^{VTA} cell intrinsic excitability. To examine OX impact on DA^{VTA} excitability, we bath applied OXA (100 nM) and measured firing elicited by brief depolarizations of constant amplitude (33) (Figure 2C, D). Whereas OXA increased firing rate in controls, it had no effect in $DA^{Ox1R\text{-}KO}$ cells (Figure 2D, E), consistent with reports showing that OXA-induced DA^{VTA} firing increase is OX_1R dependent and cell autonomous (i.e., preserved when synaptic receptors are blocked) (33). The lack of an OXA effect in $DA^{Ox1R\text{-}KO}$ mice suggests that OXA-driven OX_2R signaling does not significantly modulate DA cell firing.

Electrophysiological properties of DA^{VTA} cells lacking *Ox2R* were examined next (Figure 2F). $DA^{Ox2R\text{-}KO}$ and $DA^{Ox2R\text{-}CT}$ mice showed no differences in basal intrinsic excitability (Figure 2F, G). Strikingly, upon exposure to bath-applied OXB (2,3), DA^{VTA} neurons from control mice exhibited decreased firing (Figure 2H–J and Figure S1). This effect was abolished in $DA^{Ox2R\text{-}KO}$ mice, demonstrating the OX_2R dependency of the effect. In fact, $DA^{Ox2R\text{-}KO}$ mice's DA^{VTA} cells displayed a trend toward increased OXB-induced firing (pre- vs. post-OXB spiking: $p = .077$) (Figure 2I), potentially reflecting some level of OXB-driven OX_1R activation, despite the reported lower OXB/OX_1R affinity.

OXB-driven decreased DA^{VTA} cell firing was confirmed in wild-type mice (Figure 2K–M) and abolished by TCS-OX2-29–mediated OX_2R blockade but unaffected by ionotropic synaptic receptor blockade, ruling out indirect actions on DA^{VTA} cell excitability, e.g., by glutamatergic transmission (30). These data are consistent with dissociated cells observations, revealing opposite OXA versus OXB effects on DA^{VTA} firing and their absence, respectively, in $DA^{Ox1R\text{-}KO}$ and $DA^{Ox2R\text{-}KO}$ mice.

Dopaminergic *Ox1R* Ablation Reduces Exploration and Novelty Reactivity in an Open Field

To interrogate OX→DA neuromodulation in locomotor and exploratory behaviors, we exposed mice to an open field (OF) test (Figure 3A, left). $DA^{Ox1R\text{-}KO}$ and $DA^{Ox1R\text{-}CT}$ mice traveled similar distances across the arena (Figure 3C, left). However, $DA^{Ox1R\text{-}KO}$ mice spent more time in wall zones and less time in the arena center than controls, suggesting increased thigmotaxis (37) and anxiety-like behavior (Figure 3B, C). A small object was then placed in the OF center, and mice were allowed 5 minutes of further exploration (novel object [NO] test) (Figure 3A, right). Again, $DA^{Ox1R\text{-}KO}$ mice spent less time in the OF center and object proximity (Figure 3E). $DA^{Ox2R\text{-}KO}$ and $DA^{Ox2R\text{-}CT}$ mice showed no differences in distance traveled, times spent in wall or center zones (Figure S4A, B), or novel object exploration (Figure S4C, D). Altogether, our data reveal that dopaminergic *Ox1R*-KO enhances anxiety-like behavior during OF exploration and reduces approach toward an object placed in the OF's most anxiogenic zone.

Dopaminergic *Ox1R*-Ablated Mice Show Hyperactivity and Atypical Behavior in the EPM

Next, we evaluated $DA^{Ox1R\text{-}KO}$ mice in the EPM, commonly used to assess anxiety-like responding in rodents (Figure 3F). $DA^{Ox1R\text{-}KO}$ mice traveled a greater distance (Figure 3G) and performed more interzone crossings (Figure 3H) than controls. However, percentages of time spent in open or closed arms were unchanged (Figure 3I, J). Therefore, DA-*Ox1R*-KO induces context-dependent hyperactivity but no reduced open arm exploration. Thus, $DA^{Ox1R\text{-}KO}$ mice show misaligned anxiety-like behavioral responding in the EPM and OF tests.

Consistent with OF data, $DA^{Ox2R\text{-}KO}$ and $DA^{Ox2R\text{-}CT}$ mice did not differ in any EPM end point measures (Figure S4E–H), indicating unaltered locomotion or anxiety-like behavior.

The EPM test is considered to be a 1-trial tolerance (i.e., nonrepeatable) test, as wild-type mice run through a second EPM trial almost totally avoid open arms (38–40). Because orexinergic modulation of DA targets is critical in risk assessment (41) and executive control (18), we asked whether a second EPM exposure would reveal behavioral changes suggesting altered risk assessment, impulse control, or phobic-like open arm avoidance (42,43): 24 hours after the first EPM trial, we exposed mice to a second trial. As expected, total distance traveled was reduced between the first and second trials in all 4 genotype groups ($DA^{Ox1R\text{-}CT}$, $DA^{Ox1R\text{-}KO}$, $DA^{Ox2R\text{-}CT}$, $DA^{Ox2R\text{-}KO}$) (Figure S5). Interestingly, however, whereas $DA^{Ox1R\text{-}CT}$ mice spent less time in open arms during trial 2 compared with trial 1, $DA^{Ox1R\text{-}KO}$ mice did not (Figure 3K–L). The absence of reduced open arm occupancy in trial 2 cannot be attributed to $DA^{Ox1R\text{-}KO}$ mice's hyperactivity, as they showed similar traveled distances and number of open arm visits during trial 2 as controls (Figure S6B, D). $DA^{Ox2R\text{-}KO}$ and $DA^{Ox2R\text{-}CT}$ mice both showed the expected pattern of reduced open arm occupancy in trial 2 (Figure S4I–L).

In sum, our findings implicate DA-OX_1R signaling, but not OX_2R signaling, in context-dependent hyperactivity and anxiety-like behavior. $DA^{Ox1R\text{-}KO}$ mice's lack of reduced open arm occupancy in EPM trial 2 may reflect altered behavioral adaptation, risk assessment, and/or impulse control.

Dopaminergic *Ox1R*-Ablated Mice Exhibit Increased Impulsive and Compulsive Responding in a Reward-Driven Operant Task

$DA^{Ox1R\text{-}KO}$ mice were next exposed to the 3-CSRTT, an operant conditioning paradigm assessing reward-based learning and attention, analogous to the human continuous attention performance task (44) (Figure 4A).

As the 3-CSRTT comprises mild food restriction, body weight was monitored but indicated no intergroup differences (Figure 4B–D). $DA^{Ox1R\text{-}KO}$ and $DA^{Ox1R\text{-}CT}$ mice displayed similar 3-CSRTT learning rates (Figure 4E). However, during

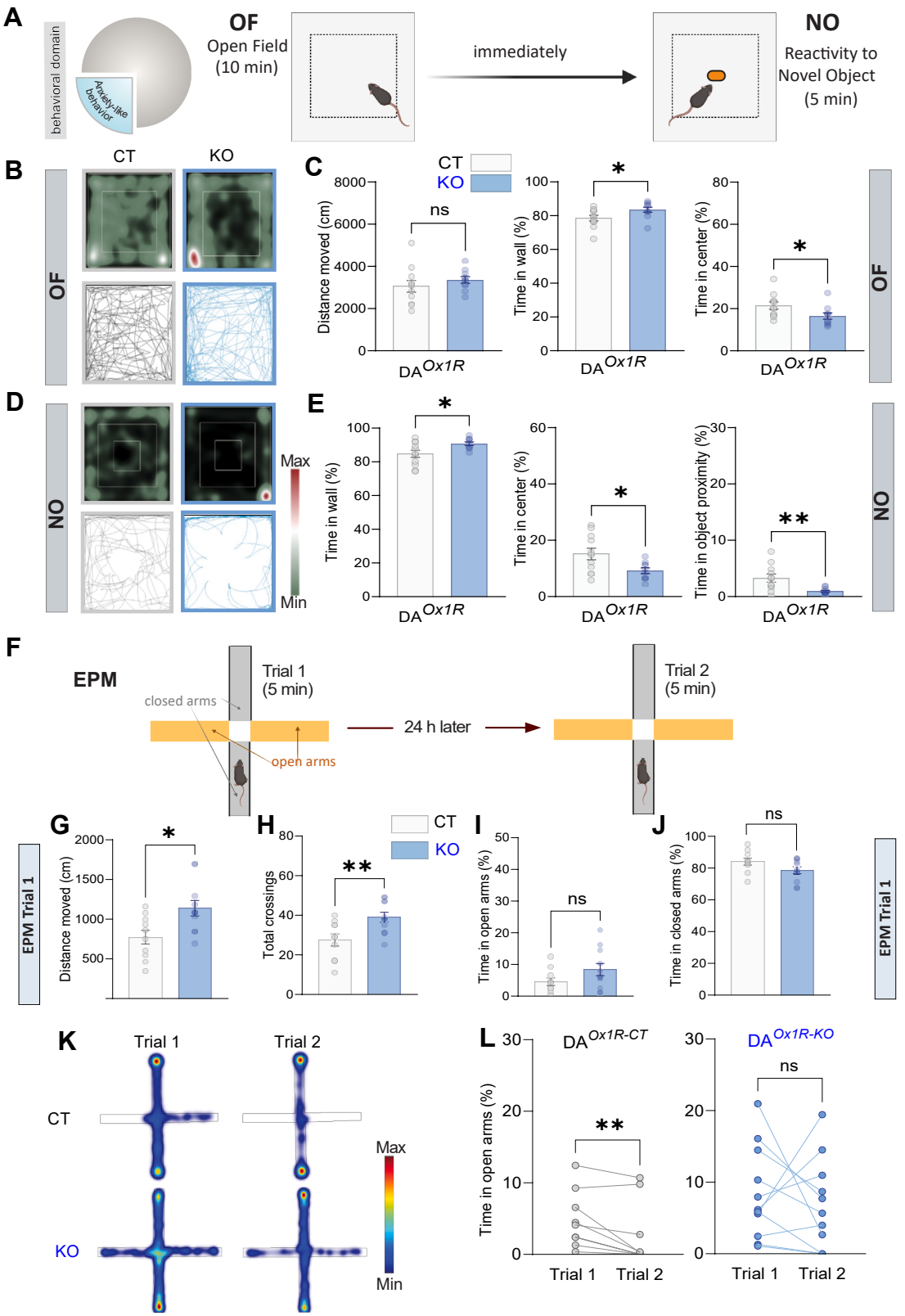

Figure 3. Dopaminergic *Ox1R*-ablated mice show reduced exploration and reactivity to novelty in an OF arena but hyperactivity and atypical responding in an EPM. $DA^{Ox1R\text{-}CT}$ and $DA^{Ox1R\text{-}KO}$ mice were subjected to the OF, reactivity to NO, and EPM tests. **(A)** Schematic design of the OF and NO tests conducted in

the first 10 training days, $DA^{Ox1R\text{-}KO}$ mice completed more total trials (Figure 4F) and premature (Figure 4K) and incorrect responses (Figure 4G) than controls, while correct responses, accuracy, and omissions were unchanged (Figure 4H–J). They also exhibited increased repetitive nosepoking in apertures (Figure 4L) and a trend toward perseverative nosepoking in the food magazine (Figure 4M), suggesting compulsivity (44).

These data assess early training, when individual mice are in different training stages depending on performance in a learning paradigm lasting several weeks. When assessed under matched training stages, no group differences appeared either under easy (stage 3) (Figure S7A–E) or challenging (stage 5) (Figure S7F–J) task contingencies, indicating that performance eventually normalizes.

As both dopaminergic $O_{x1}R$- and $O_{x2}R$-KO cause compulsivity, OXR→DA signaling appears to be protective against this trait. Interestingly, although both mutants display compulsivity, this is combined with enhanced reward learning and accuracy only in $DA^{Ox2R\text{-}KO}$ mice.

Dopaminergic *Ox1R*-Ablated Mice Show Normal Aversion-Driven Instrumental Learning

Next, we tested associative learning driven by negative affect using the active avoidance task (Figure 5A). In this 2-day task, mice learn to avoid an electric shock preceded by a 10-second tone by transiting to an adjacent chamber. $DA^{Ox1R\text{-}KO}$ mice and controls displayed similar learning, with comparable counts of avoidances (i.e., chamber transitioning during the shock-predicting tone, considered as an index of successful learning) (Figure 5D), escapes (chamber transitioning after shock onset) (Figure 5F), and premature responses (chamber transitioning preceding the tone) (Figure 5B). Premature response latencies were similar (Figure 5C), but $DA^{Ox1R\text{-}KO}$ mice exhibited briefer avoidance latencies than controls on day 1 (Figure 5E). Escape latencies were similar across genotypes on either day (Figure 5G). All $DA^{Ox1R\text{-}CT}$ mice (11/11) learned the task, while 1 of 11 $DA^{Ox1R\text{-}KO}$ mice was classified as a nonlearner (Figure 5I).

Therefore, while DA Ox_1R-KO compromises inhibitory control in positive affect–driven tasks, it does not affect negative affect–based learning. $DA^{Ox1R\text{-}KO}$ mice's faster shock-avoidance responding may reflect impulsivity, consistent with premature responding in reward-driven tasks.

Dopaminergic *Ox2R*-Ablated Mice Show Impaired Aversion-Based Instrumental Learning

While $DA^{Ox2R\text{-}KO}$ mice overperform in a reward-driven operant task (18), they severely underperformed in active avoidance, displaying fewer avoidances (i.e., chamber transitioning during the tone before shock onset) (Figure 5L), and incurred more shock exposure, since they displayed more escapes (chamber transitioning after shock onset) (Figure 5N). Premature responses were unchanged (Figure 5J).

Because task learning here is based on pain sensitivity, compromised active avoidance could result from a sensory deficit (45). However, this appears unlikely as, compared with controls, $DA^{Ox2R\text{-}KO}$ mice exhibited shorter escape latencies on day 1 (Figure 5O) and more escapes throughout (Figure 5N), suggesting that they perceived the shock but failed to learn task contingencies efficiently. When classifying mice into learners and nonlearners, only 2 of 19 controls were nonlearners (Figure 5P), while 6 of 12 $DA^{Ox2R\text{-}KO}$ mice were classified as nonlearners (Figure 5Q).

Dopaminergic *Ox2R*-Ablated Mice Show Reduced Sociability

Given the role of DA (46–48) and OX (49–51) neurons in social behavior, we tested whether dopaminergic *Ox1R*- or *Ox2R*-KO affects social interaction, using the 3-chamber sociability test, where mice explore an empty enclosure or one containing an unfamiliar juvenile mouse (Figure 6A).

$DA^{Ox1R\text{-}KO}$ mice displayed hyperlocomotion during chamber habituation, with greater distance traveled (Figure 6B) and more interchamber crossings (Figure 6C). However, during sociability testing, distance traveled was normal (Figure S8), and both $DA^{Ox1R\text{-}KO}$ and $DA^{Ox1R\text{-}CT}$ mice displayed intact sociability, spending more time near the juvenile than the empty enclosure (Figure 6E, F) and showing longer exploration bouts around the social versus inanimate stimulus (Figure 6G, H).

$DA^{Ox2R\text{-}KO}$ mice manifested no hyperlocomotion during habituation (Figure 6I, J) or sociability testing (Figure S8). However, unlike controls, they did not prefer the juvenile conspecific over the empty enclosure (Figure 6K–M) and did not show longer exploration bouts around the juvenile than the object (Figure 6N, O). Thus, our data uncover a critical role of OX_2R→DA neurotransmission in male mice sociability.

a 45 × 45 (cm) ground floor arena. Mice were allowed to explore the OF for 10 minutes. Immediately afterward, an object was placed in the arena center, and mice were allowed to explore the arena and the object for another 5 minutes (NO). The dashed-lined square delineates the center zone, defined as within 7 to 8 cm from the walls. **(B)** Heatmap (top) and trail map (bottom) of representative $DA^{Ox1R\text{-}CT}$ (left) and $DA^{Ox1R\text{-}KO}$ (right) mice during the 10-minute OF exploration. Red and green indicate maximum and minimum occupancy, respectively. **(C)** (Left) Total distance traveled in the OF for $DA^{Ox1R\text{-}CT}$ and $DA^{Ox1R\text{-}KO}$ mice ($t_{19} = 0.911$, $p = .370$, t test); (middle) time in the wall zone during the OF test ($t_{19} = 2.183$, $p = .042$, t test); (right) time in the center zone during the OF test ($t_{19} = 2.186$, $p = .041$, t test). **(D)** Heatmap (top) and trail map (bottom) of representative $DA^{Ox1R\text{-}CT}$ (left) and $DA^{Ox1R\text{-}KO}$ (right) mice during the 5-minute NO test. **(E)** (Left) time in the wall zone during the NO test ($t_{19} = 2.513$, $p = .021$, t test); (middle) time in the center zone during the NO test ($t_{19} = 2.523$, $p = .021$, t test); (right) time in the center zone at 15 cm of the NO ($t_{19} = 3.039$, $p = .007$, t test) ($n = 11$ $DA^{Ox1R\text{-}CT}$, 10 $DA^{Ox1R\text{-}KO}$). **(F)** Schematic design of the EPM test. Mice were subjected to an EPM trial for 5 minutes and, 24 hours later, reexposed to a second EPM trial for another 5 minutes. **(G)** Distance moved during EPM trial 1 revealed a higher distance traveled by $DA^{Ox1R\text{-}KO}$ vs. $DA^{Ox1R\text{-}CT}$ mice ($t_{19} = 2.777$, $p = .012$, t test) and **(H)** higher number of interzone crossings in KO vs. CT ($t_{19} = 2.931$, $p = .009$, t test). **(I)** Time in open arms ($t_{19} = 1.625$, $p = .121$) and **(J)** time in closed arms ($t_{19} = 1.790$, $p = .089$, t test) did not significantly differ between KO and CT. **(K)** Representative heatmaps depicting location of a $DA^{Ox1R\text{-}CT}$ (top) and a $DA^{Ox1R\text{-}KO}$ mouse (bottom) during EPM trials 1 and 2. Heatmap occupancy color scale from red (maximum) to dark blue (minimum). **(L)** $DA^{Ox1R\text{-}CT}$ mice spent less time in open arms during EPM trial 2 than trial 1, as is commonly observed in rodents ($W = -51$, $p = .006$, Wilcoxon test). In contrast, $DA^{Ox1R\text{-}KO}$ mice did not spend less time in open arms during EPM trial 2 relative to trial 1 ($t_{10} = 0.652$, $p = .530$, paired t test). Bar graphs depict mean ± SEM ($n = 10$ $DA^{Ox1R\text{-}CT}$, $n = 11$ $DA^{Ox1R\text{-}KO}$). $^*p < .05$, $^{**}p < .01$. CT, control genotype mouse group; DA, dopamine; EPM, elevated plus maze; KO, knockout genotype mouse group; NO, novel object; OF, open field.

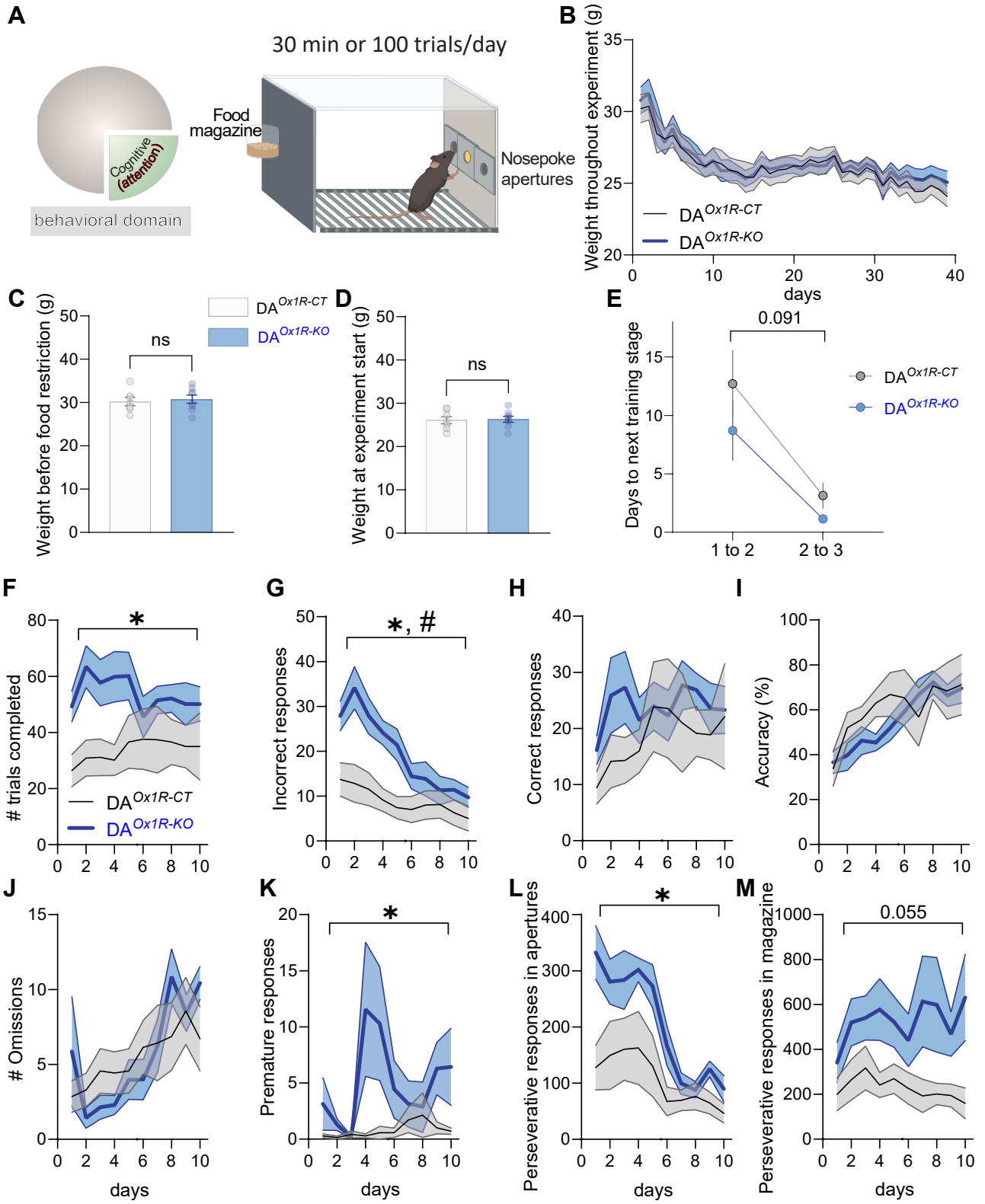

Figure 4. Dopaminergic *Ox1R*-ablated mice exhibit impulsive- and compulsive-like behaviors in reward-driven operant conditioning. Performance of $DA^{Ox1R\text{-}KO}$ (KO) and $DA^{Ox1R\text{-}CT}$ (CT) mice in the 3-CSRTT. **(A)** Schematic of the 3-CSRTT operant chamber. Three nosepoking apertures were located on the wall opposite the food magazine dispensing the chocolate-flavored sucrose pellet rewards. **(B)** Timeline of body weight throughout the 3-CSRTT procedure

DISCUSSION

Both OX and DA neurons are neural hubs encoding past and current salient information critical to adaptive regulation of arousal, motivation, and stress. While $OX^{LHA} \rightarrow DA^{VTA}$ connectivity appears central for reward- and aversion-driven behaviors relevant to motivational states and neuropsychiatric disorders (11,22–24), differential modulation by OX_1Rs versus OX_2Rs within this pathway remains poorly defined.

Therefore, we generated mice with DA-specific loss of *Hcrtr1/Ox1R* or *Hcrtr2/Ox2R* and examined $OX \rightarrow DA$ circuit function across behavioral domains. Given DA^{VTA} neurons' central role in OX/DA interactions, we interrogated DA^{VTA} underlying electrophysiology and uncovered profoundly divergent orexinergic modulation of DA^{VTA} cell activity and function by OX_1Rs versus OX_2Rs (Figure 7).

$DA^{Ox1R\text{-}KO}$ Mouse Behavior: Anxiety and Hypermotricity

$DA^{Ox1R\text{-}KO}$ mice showed context-dependent hyperactivity, impulsivity, and repetitive behaviors, as evidenced by increased distance traveled and interzone crossings in the EPM and 3-chamber assays; elevated trial number; and premature, incorrect, and perseverative responses during 3-CSRTT acquisition. Exploratory behavior was increased compared with controls in confined arenas (EPM, 3 chamber) but reduced in the OF, consistent with anxiety-like behavior. This was not mirrored in the EPM, where open arm occupancy was unchanged. Such OF/EPM dissociation has been reported previously (52) and may reflect differences in habituation, temporospatial configuration, or end point measures (53). Occlusion of the EPM trial 2 1-trial tolerance effect suggests altered behavioral adaptation or risk assessment.

Reduced OF exploration contrasts with the findings of Xiao *et al.* (54). This discrepancy likely reflects model differences: Our mice express *Hcrtr1* and *Hcrtr2* in >80% of ventral midbrain tyrosine hydroxylase–positive neurons (18) and use a $Dat^{+/ires\text{-}Cre}$ driver with normal DA levels (55) and locomotion (56), whereas Xiao *et al.*'s (54) used $Dat^{+/Cre}$ mice with reduced *Dat* expression, increasing DA levels, and hyperlocomotion (57,58). Arena size may also contribute (27 × 27 cm vs. in our case 45 × 45 cm) to different outcomes. Strengthening this interpretation, although $DA^{Ox1R\text{-}KO}$ mice show reduced OF exploration, they show hyperactivity in confined arenas.

Task-locked DA-sensor photometry in the NAc and mPFC should clarify the mechanisms underlying $DA^{Ox1R\text{-}KO}$ mice's behavioral deficits. Altered OX_1R-dependent DA release in mesocortical ($DA^{VTA} \rightarrow$ mPFC) and/or mesolimbic ($DA^{VTA} \rightarrow$ NAc) pathways may be involved. Hyperactivity, altered exploration, premature and repetitive responses, and faster avoidance could reflect inefficient saliency processing due to altered $DA^{VTA} \rightarrow$ mPFC signaling, causing suboptimal goal-directed behavior and motor output (59–62). Meanwhile, DA^{VTA} projections to the NAc and basolateral amygdala are implicated in fear extinction (63,64); thus, lower activity in mesolimbic pathways could promote anxiety states.

$DA^{Ox2R\text{-}KO}$ Mouse Behavior: Constitutively Hyperaroused, Strong in Reward-Based but Compromised in Avoidance-Driven Learning and Sociability

DA-specific *Ox2R* loss yields a mixed phenotype combining strengths and weaknesses. Mice show elevated electrocortical alertness markers, enhanced theta-gamma coupling, and improved learning and attention in reward-driven operant tasks (18) but impaired impulse control (18) and severely compromised aversion-based learning. Thus, DA OX_2R-dependent hyperarousal benefits processing of positive stimuli but impairs responses to negative cues, indicating distinct effector pathways for reward versus aversive learning. Comparable trade-offs occur across strains: C57BL/6 mice excel in reward-driven tasks but underperform in aversive tasks, whereas DBA/2J mice display heightened anxiety and moderate avoidance learning but diminished reward motivation, reflecting reward-sensitive versus punishment-sensitive cognitive styles (65,66).

$DA^{Ox2R\text{-}KO}$ mice's enhanced 3-CSRTT performance may reflect disinhibition of DA^{VTA} neurons, thereby increasing attentional engagement with reward-predictive cues. DA^{VTA}

showed no difference between KO and CT groups (time: $F_{38,494} = 19.881$, $p < .001$; genotype: $F_{1,13} = 0.061$, $p = .808$; time × genotype: $F_{38,494} = 0.363$, $p = 1.000$, repeated-measures 2-way ANOVA). **(C)** Body weight of $DA^{Ox1R\text{-}KO}$ and $DA^{Ox1R\text{-}CT}$ mice before food restriction ($t_{13} = 0.417$, $p = .683$, *t* test) and **(D)** at 3-CSRTT procedure start ($t_{13} = 0.200$, $p = .844$, *t* test) did not differ ($n = 7$ $DA^{Ox1R\text{-}CT}$, 8 $DA^{Ox1R\text{-}KO}$). **(E)** $DA^{Ox1R\text{-}KO}$ mice showed a tendency to learn faster than $DA^{Ox1R\text{-}CT}$ mice during initial training days (training stages 1–3), as shown by comparing the number of days to reach the next training stage (time: $F_{1,12} = 15.517$, $p = .002$; genotype: $F_{1,12} = 1.827$, $p = .201$; time × genotype interaction: $F_{1,12} = 3.379$, $p = .091$, repeated-measures 2-way ANOVA). **(F)** $DA^{Ox1R\text{-}KO}$ mice completed more total trials than $DA^{Ox1R\text{-}CT}$ littermates (time: $F_{2.625,31.497} = 0.653$, $p = .567$; genotype: $F_{1,12} = 5.235$, $p = .041$; time × genotype interaction: $F_{2.625,31.497} = 1.183$, $p = .328$; repeated-measures 2-way ANOVA) and **(G)** more incorrect responses during the initial 10 training days (time: $F_{3.551,42.611} = 14.670$, $p < .001$; genotype: $F_{1,12} = 8.389$, $p = .013$; time × genotype: $F_{3.551,42.611} = 4.413$, $p = .006$; repeated-measures 2-way ANOVA). However, $DA^{Ox1R\text{-}KO}$ mice did not differ from $DA^{Ox1R\text{-}CT}$ mice in **(H)** number of correct responses (time: $F_{1.977,23.719} = 1.614$, $p = .220$; genotype: $F_{1,12} = 0.863$, $p = .371$; time × genotype: $F_{1.977,23.719} = 0.762$, $p = .476$; repeated-measures 2-way ANOVA) or **(I)** response accuracy (time: $F_{2.372,28.461} = 8.731$, $p < .001$; genotype: $F_{1,12} = 0.320$, $p = .582$; time × genotype: $F_{2.372,28.461} = 1.258$, $p = .304$; repeated-measures 2-way ANOVA) or **(J)** number of omissions (time: $F_{2.630,31.563} = 5.033$, $p = .008$; genotype: $F_{1,12} = 0.009$, $p = .928$; time × genotype: $F_{2.630,31.563} = 1.380$, $p = .268$; repeated-measures 2-way ANOVA) during the first 10 training days. **(K)** $DA^{Ox1R\text{-}KO}$ mice exhibited more premature responses than $DA^{Ox1R\text{-}CT}$ mice during the first 10 training days (time: $F_{2.175,26.100} = 1.573$, $p = .226$; genotype: $F_{1,12} = 5.775$, $p = .033$; time × genotype: $F_{2.175,26.100} = 1.767$, $p = .189$; repeated-measures 2-way ANOVA), **(L)** more repetitive nosepoking responses in any of the 3 apertures (time: $F_{3.456,41.468} = 13.310$, $p < .001$; genotype: $F_{1,12} = 6.294$, $p = .027$; time × genotype: $F_{3.456,41.468} = 2.478$, $p = .067$; repeated-measures 2-way ANOVA), and **(M)** a trend toward a higher number of repetitive nosepoking responses in the food magazine (time: $F_{2.753,33.031} = 1.451$, $p = .247$; genotype: $F_{1,12} = 4.501$, $p = .055$; time × genotype: $F_{2.753,33.031} = 1.677$, $p = .194$; repeated-measures 2-way ANOVA). Bar graphs and timelines depict mean ± SEM ($n = 7$ $DA^{Ox1R\text{-}CT}$, 7 $DA^{Ox1R\text{-}KO}$). * denotes a significant genotype effect, and # denotes a significant time × genotype effect in repeated-measures 2-way ANOVA. 3-CSRTT, 3-choice serial reaction time task; ANOVA, analysis of variance; CT, control genotype mouse group; DA, dopamine; KO, knockout genotype mouse group.

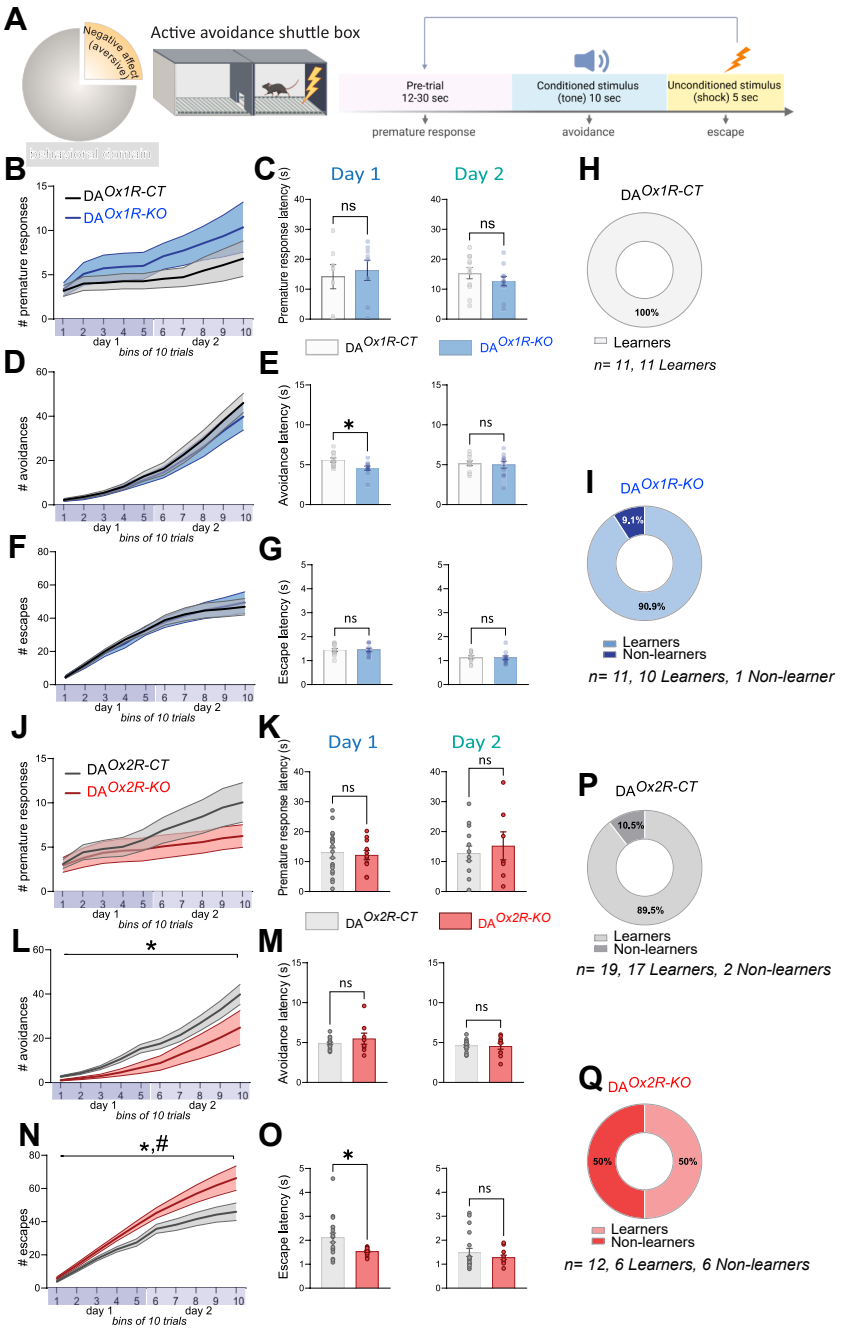

Figure 5. Dopaminergic *Ox2R*-ablated mice show impaired aversion-driven instrumental learning. Performance of $DA^{Ox1R\text{-}KO}$ vs. $DA^{Ox1R\text{-}CT}$ and $DA^{Ox2R\text{-}KO}$ vs. $DA^{Ox2R\text{-}CT}$ mice in an active avoidance task. **(A)** Schematic of the active avoidance shuttle box and experimental design. An interchamber run during the pretrial is a premature response, an interchamber run during the tone is an avoidance response (indicative of successful learning), and an interchamber run during the shock is an escape response. **(B)** Numbers of premature responses did not differ between $DA^{Ox1R\text{-}CT}$ and $DA^{Ox1R\text{-}KO}$ mice across the 2 testing days (time: $F_{1.233,24.668} = 7.511$, $p < .001$; genotype: $F_{1,20} = 1.374$, $p = .255$; time × genotype: $F_{1.233,24.668} = 0.878$, $p = .380$; repeated-measures 2-way ANOVA). **(C)** Similar premature response latencies in $DA^{Ox1R\text{-}CT}$ and $DA^{Ox1R\text{-}KO}$ mice (day 1, left: $t_{13} = 0.400$, $p = .695$; day 2, right: $t_{20} = 1.082$, $p = .292$; *t* tests). **(D)** Numbers of avoidance responses did not differ between $DA^{Ox1R\text{-}CT}$ and $DA^{Ox1R\text{-}KO}$ mice across the 2 testing days (time: $F_{1.126,22.519} = 97.899$, $p < .001$; genotype: $F_{1,20} = 0.369$, $p = .550$; time × genotype: $F_{1.126,\ 22.519} = 0.502$, $p = .507$; repeated-measures 2-way ANOVA). **(E)** $DA^{Ox1R\text{-}KO}$ mice showed shorter avoidance response latencies than $DA^{Ox1R\text{-}CT}$ mice on the first testing day, indicating a faster avoidance response (day 1, left: $t_{20} = 2.796$, $p = .011$; day 2, right: $t_{20} = 0.290$, $p = .775$; *t* tests). **(F)** Number of escape responses did not differ between $DA^{Ox1R\text{-}CT}$ and $DA^{Ox1R\text{-}KO}$ mice across the 2 testing days (time: $F_{1.156,23.113} = 102.588$, $p < .001$; genotype: $F_{1,20} = 0.003$, $p = .960$; time × genotype: $F_{1.156,23.113} = 0.200$, $p = .695$; repeated-measures 2-way ANOVA). **(G)** Similar escape response latencies in $DA^{Ox1R\text{-}CT}$ and $DA^{Ox1R\text{-}KO}$ mice (day 1, left: $t_{20} = 0.048$, $p = .962$; day 2, right: $U = 51.50$, $p = 0.573$; *t* test and Mann-Whitney test, respectively). **(H, I)** Pie charts of learners vs. nonlearners in $DA^{Ox1R\text{-}CT}$ and $DA^{Ox1R\text{-}KO}$ mice show that both genotypes learned efficiently (n = 11 $DA^{Ox1R\text{-}CT}$, 11 $DA^{Ox1R\text{-}KO}$). **(J)** Numbers of premature responses did not differ between $DA^{Ox2R\text{-}CT}$ and $DA^{Ox2R\text{-}KO}$ mice across the 2 testing days (time: $F_{1.303,37.779} = 12.325$, $p < .001$; genotype: $F_{1,29} = 0.744$, $p = .396$; time × genotype: $F_{1.303,37.779} = 2.178$, $p = .143$; repeated-measures 2-way ANOVA). **(K)** Similar premature response latencies in $DA^{Ox2R\text{-}CT}$ and $DA^{Ox2R\text{-}KO}$ mice (day 1, left: $t_{28} = 0.290$, $p = .774$; day 2, right: $t_{18} = 0.528$, $p = .604$; *t* tests). **(L)** $DA^{Ox2R\text{-}KO}$ mice show a decreased number of avoidance responses compared with $DA^{Ox2R\text{-}CT}$ mice across the 2 testing days (time: $F_{1.146,33.242} = 46.938$, $p < .001$; genotype: $F_{1,29} = 4.507$, $p = .042$; time × genotype: $F_{1.146,33.242} = 2.084$, $p = .156$; repeated-measures 2-way ANOVA). **(M)** Similar avoidance response latencies in $DA^{Ox2R\text{-}CT}$ and $DA^{Ox2R\text{-}KO}$ mice (day 1, left: $t_{24} = 1.185$, $p = .248$; day 2, right: $t_{25} = 0.111$, $p = .912$; *t* tests). **(N)** $DA^{Ox2R\text{-}KO}$ mice show a higher number of escapes (interchamber run after shock exposure) than $DA^{Ox2R\text{-}CT}$ mice, with both genotype and time × genotype significant effects (time: $F_{1.286,37.284} = 126.005$, $p < .001$; genotype: $F_{1,29} = 6.354$, $p = .017$; time × genotype: $F_{1.286,\ 37.284} = 3.833$, $p = .048$; repeated-measures 2-way ANOVA). **(O)** $DA^{Ox2R\text{-}KO}$ mice nevertheless show shorter escape response latencies than $DA^{Ox2R\text{-}CT}$ mice on the first testing day, suggesting that they are sensitive to the electric shock (day 1, left: $U = 62$, $p = .035$; day 2, right: $U = 113$, $p = .984$; Mann-Whitney tests). **(P, Q)** Pie charts of learners vs. nonlearners in $DA^{Ox2R\text{-}CT}$ and $DA^{Ox2R\text{-}KO}$ mice highlight the markedly reduced learning efficiency observed among $DA^{Ox2R\text{-}KO}$ mice. Bar graphs and timelines depict mean ± SEM (n = 19 $DA^{Ox2R\text{-}CT}$, 12 $DA^{Ox2R\text{-}KO}$). * denotes a significant genotype effect, and # denotes a significant time × genotype effect in repeated-measures 2-way ANOVA. ANOVA, analysis of variance; CT, control genotype mouse group; DA, dopamine; KO, knockout genotype mouse group; ns, nonsignificant.

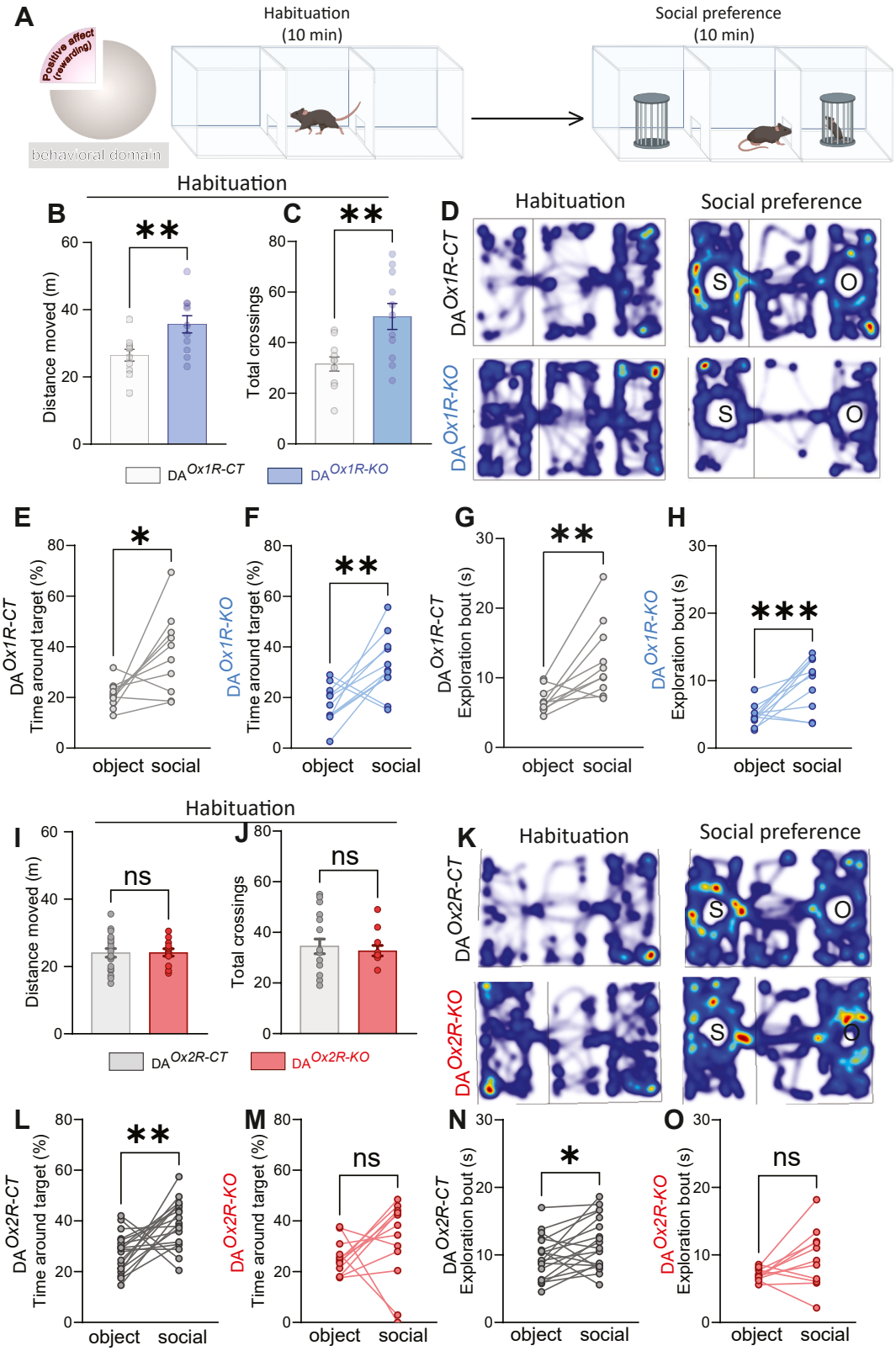

Figure 6. Dopaminergic *Ox2R*-ablated mice show reduced sociability. Social preference of $DA^{Ox1R\text{-}KO}$ and $DA^{Ox2R\text{-}KO}$ mice was probed against their respective genetic controls using the 3-chamber test. **(A)** Schematic of the experimental design consisting of 2 phases 1) a 10-minute habituation phase

activation may in turn enhance NAc DA release, and because DA inhibits $D2^{NAc}$ cells involved in learned risk avoidance (67), this may contribute to mice's active avoidance deficits. It should be noted that direct OX→$D2^{NAc}$ excitation contributes to innate risk avoidance (41) and may also contribute to learned avoidance.

The neocortex is also an area where OX-DA interactions are prominent (68,69). Stimulating D1aR-expressing, OX_2R-responding layer 6b neurons (70,71) boosts neocortical excitability (72), while silencing them causes anxiolytic effects (69). Altered OX_2R→DA transmission may also impact intracortical activity by affecting presynaptic DA release (73,74).

$DA^{Ox2R\text{-}KO}$ mice display endophenotypes reminiscent of autism spectrum disorder (ASD): selective learning enhancement, compulsivity, and social interaction difficulties (75–79). Prior studies implicated OX neurons in social behavior (49,80) but lacked cell-type specificity. Here we showed that DA-selective *Ox$_2$R*-KO, but not *Ox$_1$R*-KO, reduced time spent interacting with a conspecific. Using mice as ASD models is debated (76,77); nevertheless, altered DA^{VTA}→NAc/mPFC pathways are implicated in ASD-related traits (78,79), and probing DA release in these circuits in $DA^{Ox2R\text{-}KO}$ mice may highlight underlying circuitry.

Compulsivity and impulsivity-like endophenotypes were the only behavioral traits that we found in both $DA^{Ox1R\text{-}KO}$ and $DA^{Ox2R\text{-}KO}$ mice. Impaired executive control in the form of premature or repetitive responding may represent a converging effect of disrupting OX→DA pathways.

Linking Mouse Behavioral Profiles With Ex Vivo DA^{VTA} Cell Electrophysiology

$DA^{Ox1R\text{-}KO}$ and $DA^{Ox2R\text{-}KO}$ mice's contrasting behaviors suggest distinct contributions of OX_1Rs and OX_2Rs to DA cell activity and synaptic circuits. Our patch-clamp recordings using dissociated DA^{VTA} neurons or intact slices revealed opposing OXA versus OXB effects. OXA increased DA^{VTA} firing in wild-type and $DA^{Ox1R\text{-}CT}$, but not $DA^{Ox1R\text{-}KO}$, mice indicating that, although OXA is reported to bind equally well to OX_1Rs and OX_2Rs, OXA responses are primarily OX_1R driven, consistent with blockade by OX_1R antagonists (33). In contrast, OXB and the OX_2R-selective agonist OXB-AL induced OX_2R-dependent inhibition. The OXB-mediated firing decrease was abolished in $DA^{Ox2R\text{-}KO}$ mice, with a trend toward increased firing, likely reflecting residual OX_1R activation by OXB. Stronger inhibition by OXB-AL and YNT-185 than by OXB supports this interpretation.

In sum, OXA→OX_1R signaling stimulates DA^{VTA} neurons, while OXB→OX_2R signaling inhibits them. *Ox2R* deletion–mediated disinhibition thus facilitates excitatory effects, consistent with $DA^{Ox2R\text{-}KO}$ mice theta-enriched wakefulness (18). OX_1Rs may promote reward-related behaviors, while OX_2Rs restrain overexcitation to maintain behavioral flexibility.

Our findings contrast with reports (28) of DA^{VTA} excitation by both OXA and OXB in rat slices. However, these authors recorded spontaneous firing, reflecting both intrinsic and network inputs, whereas we stimulated DA^{VTA} cells to fire at regular intervals, thus isolating intrinsic excitability in response to OXs.

Intracellular mechanisms whereby OX_2R signaling is intrinsically inhibitory in DA^{VTA} neurons remain to be elucidated. Although OX_2R signaling is excitatory in various cell types, such as histaminergic neurons (81), OXR signaling is cell specific (82), and inhibition has been reported in pro-opiomelanocortin-expressing neurons, suprachiasmatic nucleus neurons, and some melanin-concentrating hormone–producing neurons (83–86). Given DA^{VTA} neuron relatively depolarized V_m (87), reduced spiking could arise from modulation of K^+ channels active near spike threshold. OX_2Rs couple to both $G\alpha_q$ and $G\alpha_{i/o}$ (82), which can modulate K^+ currents (88). $G\alpha_q$-dependent Ca^{2+} mobilization may activate SK/K_{Ca} channels (89), expressed in DA^{VTA} neurons (90) and implicated in autistic-like traits (91). $G\beta\gamma$ subunits may modulate potassium

during which the mouse is allowed to freely explore the arena, and 2) a subsequent 10-minute social preference phase during which 2 grided enclosures are located in 2 opposite chambers, 1 empty and 1 containing a same-sex unfamiliar juvenile mouse, and the experimental mouse is allowed to freely explore the 3 chambers and interact with the juvenile using olfactory, visual, auditory, and tactile cues. During habituation, $DA^{Ox1R\text{-}KO}$ mice **(B)** traveled across a longer distance (t_{20} = 2.972, p = .007, t test; n = 11 $DA^{Ox1R\text{-}CT}$, 11 $DA^{Ox1R\text{-}KO}$) and **(C)** performed more interzone crossings relative to $DA^{Ox1R\text{-}CT}$ mice (t_{20} = 3.224, p = .004, t test; n = 11 $DA^{Ox1R\text{-}CT}$, 11 $DA^{Ox1R\text{-}KO}$). **(D)** Representative heatmaps of location of a $DA^{Ox1R\text{-}CT}$ and a $DA^{Ox1R\text{-}KO}$ mouse during habituation (left) and social preference (right) phases. "S" denotes the social stimulus–containing enclosure, and "O" denotes the object (empty) enclosure. Both $DA^{Ox1R\text{-}CT}$ **(E)** and $DA^{Ox1R\text{-}KO}$ **(F)** mice spent a higher percentage of the total time within proximity to the social than the inanimate target (main effect of stimulus: $F_{1,19}$ = 18.318, $p < .001$; main effect of genotype: $F_{1,19}$ = 1.736, p = .203; genotype × stimulus interaction: $F_{1,19}$ = 0.006, p = .940; mixed 2-way ANOVA, followed by post hoc paired t tests: $DA^{Ox1R\text{-}CT}$: t_9 = 2.840, p = .019; $DA^{Ox1R\text{-}KO}$: t_{10} = 3.230, p = .009). Both $DA^{Ox1R\text{-}CT}$ **(G)** and $DA^{Ox1R\text{-}KO}$ **(H)** mice displayed longer exploration bouts within proximity to the social than the inanimate target (main effect of stimulus: $F_{1,19}$ = 28.254, $p < .001$; main effect of genotype: $F_{1,19}$ = 3.812, p = .066; genotype × stimulus interaction: $F_{1,19}$ = 0.130, p = .722; mixed 2-way ANOVA, followed by post hoc paired t tests: $DA^{Ox1R\text{-}CT}$: t_9 = 3.564, p = .006; $DA^{Ox1R\text{-}KO}$: t_{10} = 3.987, p = .003) (n = 10 $DA^{Ox1R\text{-}CT}$, 11 $DA^{Ox1R\text{-}KO}$). In contrast to $DA^{Ox1R\text{-}KO}$ mice, during habituation, $DA^{Ox2R\text{-}KO}$ mice did not exhibit differences in distance traveled **(L)** or in the number of interchamber crossings **(J)** compared with $DA^{Ox2R\text{-}CT}$ mice (total distance moved: $DA^{Ox2R\text{-}CT}$ vs. $DA^{Ox2R\text{-}KO}$, t_{29} = 0.065, p = .949, t test; n = 19 $DA^{Ox2R\text{-}CT}$, 12 $DA^{Ox2R\text{-}KO}$; total interchamber crossings: $DA^{Ox2R\text{-}CT}$ vs. $DA^{Ox2R\text{-}KO}$, U = 110.5, p = .897, Mann-Whitney test; n = 19 $DA^{Ox2R\text{-}CT}$, 12 $DA^{Ox2R\text{-}KO}$). **(K)** Representative heatmaps of a $DA^{Ox2R\text{-}CT}$ and a $DA^{Ox2R\text{-}KO}$ mouse during habituation (left) and social preference (right). Analysis of social preference in $DA^{Ox2R\text{-}CT}$ and $DA^{Ox2R\text{-}KO}$ mice revealed that while control mice show normal social preference **(L)**, $DA^{Ox2R\text{-}KO}$ mice spend similar times exploring the juvenile and inanimate object **(M)** (main effect of stimulus: $F_{1,29}$ = 9.140, p = .005; main effect of genotype: $F_{1,29}$ = 4.949, p = .034; genotype × stimulus interaction: $F_{1,29}$ = 0.748, p = .394; mixed 2-way ANOVA, followed by post hoc paired t tests: $DA^{Ox2R\text{-}CT}$, t_{18} = 3.386, p = .003; $DA^{Ox2R\text{-}KO}$, W = 30.00, p = .266, Wilcoxon test). Moreover, $DA^{Ox2R\text{-}CT}$ mice show longer average exploration bouts for the social than for the inanimate target **(N)**, whereas $DA^{Ox2R\text{-}KO}$ mice showed only a trend **(O)** (main effect of stimulus: $F_{1,28}$ = 7.818, p = .009; main effect of genotype: $F_{1,28}$ = 5.094, p = .032; genotype × stimulus interaction: $F_{1,28}$ = 0.050, p = .825; mixed 2-way ANOVA, followed by post hoc paired t tests: $DA^{Ox2R\text{-}CT}$: t_{18} = 2.393, p = .028; $DA^{Ox2R\text{-}KO}$: t_{10} = 1.927, p = .083). Bar graphs show individual values and mean ± SEM (n = 19 $DA^{Ox2R\text{-}CT}$, 12 $DA^{Ox2R\text{-}KO}$). $^*p < .05$, $^{**}p < .01$, $^{***}p < .001$. ANOVA, analysis of variance; CT, control genotype mouse group; DA, dopamine; KO, knockout genotype mouse group; ns, nonsignificant.

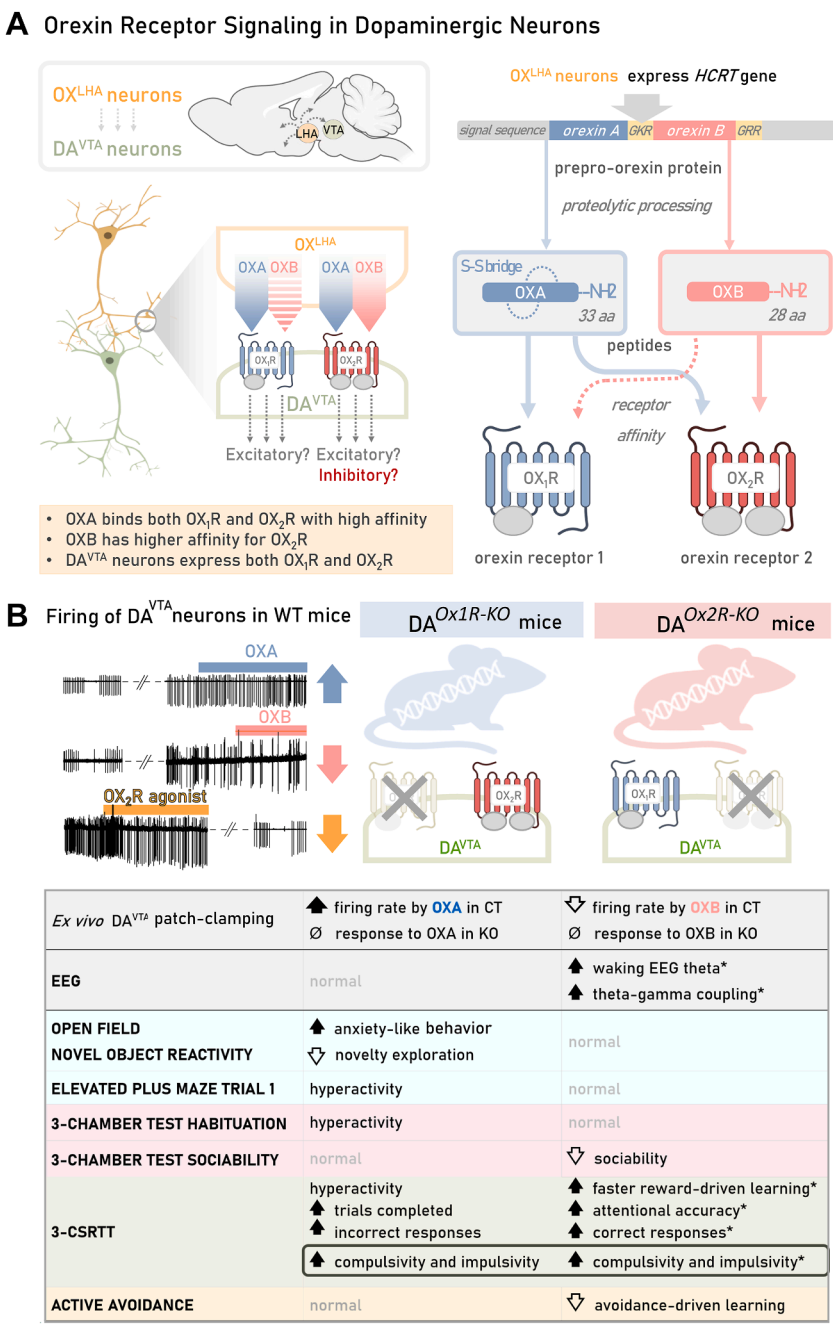

Ex vivo DA^{VTA} patch-clamping	▲ firing rate by **OXA** in CT Ø response to OXA in KO	▽ firing rate by OXB in CT Ø response to OXB in KO
EEG	normal	▲ waking EEG theta* ▲ theta-gamma coupling*
OPEN FIELD **NOVEL OBJECT REACTIVITY**	▲ anxiety-like behavior ▽ novelty exploration	normal
ELEVATED PLUS MAZE TRIAL 1	hyperactivity	normal
3-CHAMBER TEST HABITUATION	hyperactivity	normal
3-CHAMBER TEST SOCIABILITY	normal	▽ sociability
3-CSRTT	hyperactivity ▲ trials completed ▲ incorrect responses	▲ faster reward-driven learning* ▲ attentional accuracy* ▲ correct responses*
	▲ compulsivity and impulsivity	▲ compulsivity and impulsivity*
ACTIVE AVOIDANCE	normal	▽ avoidance-driven learning

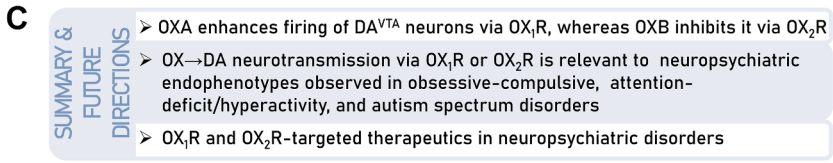

Figure 7. Summary schematic depiction of divergent neuromodulation of dopaminergic neurons by hypocretin/orexin receptors 1 and 2 as reflected at electrophysiological and behavioral levels. **(A)** $OX^{LHA} \rightarrow DA^{VTA}$ neurotransmission. **(B)** $DA^{Ox1R\text{-}KO}$ and $DA^{Ox2R\text{-}KO}$ mice exhibit widely distinct DA^{VTA} electrophysiological, EEG brain activity, and behavioral phenotypes. However, both show enhanced compulsivity- and impulsivity-like behaviors. **(C)** Summary and future directions. Asterisks denote data from Bandarabadi *et al.* (18). 3-CSRTT, 3-choice serial reaction time task; aa, amino acids; CT, control genotype mouse group; DA, dopamine; EEG, electroencephalography; GKR, glycine-lysine-arginine; GRR, glycine-arginine-arginine; KO, knockout genotype mouse group; LHA, lateral hypothalamic area; OX_1R, orexin receptor 1; OX_2R, orexin receptor 2; OXA, orexin A; OXB, orexin B; S-S bridge, disulfide bridge; VTA, ventral tegmental area; WT, wild-type.

voltage-gated channel subfamily Q (KCNQ) channels (92,93), while $G_i\beta\gamma$ can activate inwardly rectifying K^+ channels, as in DA^{VTA} cell D_2 autoreceptor–mediated inhibition (94).

Limitations

While we use pan-neuronal (*Dat*-driven) mouse models, our electrophysiological analyses focus on DA^{VTA} neurons as well-

characterized OX targets involved in behavioral end points of interest. Other DA populations, including nigral, hypothalamic, and dorsal raphe DA neurons (95–100), may also contribute to observed phenotypes if they express *Ox$_1$R* and/or *Ox$_2$R*. DA cell heterogeneity in receptor expression, electrophysiology, and connectivity confounds interpretation of all pan-DA studies (101). Moreover, developmental compensation may occur, with *OxR* inactivation happening at ∼embryonic day 17 (55), while OX neurons mature postnatally (102). Adult-specific, nucleus-targeted Cre delivery should clarify this.

Only male mice were studied. Given sexual dimorphism in OX- and DA-mediated behaviors (49,103,104), females may show distinct phenotypes (105). Females show heightened OX activation, contributing to different stress responses and cognitive flexibility (103), traits relevant to neuropsychiatric conditions disproportionately affecting women. Inclusion of females will enable better understanding of the mechanisms underlying sex-specific vulnerabilities in OX- and DA-dependent disorders.

Implications for Neuropsychiatry

We identified a genetically defined link between direct OX→DA neurotransmission and socioemotional and executive functions, revealing a receptor-specific dichotomy in DA^{VTA} regulation: OXB suppresses DA neuron activity via OX_2Rs, whereas OXA increases excitability via OX_1Rs. These findings may be relevant to mechanisms underlying obsessive-compulsive disorder (OCD), attention-deficit/hyperactivity disorder, and ASD.

With ongoing development of OXR-targeted therapeutics—selective and dual agonists/antagonists for substance abuse, eating, OCD, anxiety, pain, and sleep disorders (9,94,106–109)—understanding receptor-specific effects is essential. Dual OXR antagonists, used for insomnia and explored for opioid addiction (107), may exacerbate compulsivity/impulsivity, enhanced in $DA^{Ox1R\text{-}KO}$ and $DA^{Ox2R\text{-}KO}$ mice. OX_1R-selective antagonists may treat addiction or compulsive disorders without promoting sleep (110), but DA-*Ox1R*-KO–induced anxiety suggests potential anxiogenic effects.

As OXB and OX_2R agonists reduce DA^{VTA} excitability, monitoring DA-related traits in subjects treated with OX_2R-selective agonists for narcolepsy or obstructive sleep apnea is critical. Because DA^{VTA} neuron–inhibiting D_2 agonists aggravate cataplexy (111), similar effects could be anticipated; however, OX_2R agonist TAK-861 8-week trial in NT1 reported cataplexy improvement (112,113), suggesting limited dopaminergic circuit engagement in current therapeutic contexts. Whether prolonged OX_2R agonism induces anhedonia via sustained DA^{VTA} suppression (114) is unknown. Overall, these findings have broad implications for emerging OXR neuropharmacology.

ACKNOWLEDGMENTS AND DISCLOSURES

This work was supported by the Swiss National Science Foundation (Grant No. 31003A_182613 [to AV]) and by the University of Milano-Bicocca (postdoctoral fellowship [to LCG], Grant Nos. 2021-ATE-0042 and 2024-ATE-0117 [to AB]).

We thank Dr. Leonardo Restivo from the NeuroBau Behavioral Facility at the Department of Fundamental Neurosciences of the University of Lausanne for help, notably in active avoidance testing, and Anne-Catherine Thomas for mouse genotyping.

ST, SA, LCG, FG, AV, AB, and MT conceived the study. ST performed and analyzed behavioral experiments with the help of RK and SR for 3-CSRTT experimentation. SA performed and analyzed patch-clamp recordings of DA cells in brain slices. LCG, FG, and AB performed and analyzed patch-clamp recordings of dissociated DA cells. GL contributed to study interpretation and figure design. AV generated *Hcrtr1* and *Hcrtr2* floxed and whole-body KO mouse lines. AV, AB, and MT supervised the project. All authors contributed to article editing and figure design.

A previous version of this article was published as a preprint on bioRxiv: https://www.biorxiv.org/content/10.1101/2025.02.14.638329v1.

The authors report no biomedical financial interests or potential conflicts of interest.

ARTICLE INFORMATION

From the Department of Biomedical Sciences, University of Lausanne, Lausanne, Switzerland (ST, RK, SR, GL, MT, AV); Laboratory of Behavioral Genetics, Brain Mind Institute, École Polytechnique Fédérale de Lausanne, Lausanne, Switzerland (SA); and Department of Biotechnology and Biosciences and NeuroMI (Milan Center of Neuroscience), University of Milano-Bicocca, Milano, Italy (LCG, FG, AB).

Address correspondence to Anne Vassalli, Ph.D., at Anne.Vassalli@unil.ch.

Received Jul 20, 2025; revised Apr 28, 2026; accepted May 29, 2026.

Supplementary material cited in this article is available online at https://doi.org/10.1016/j.biopsych.2026.05.022.

REFERENCES

1. Mahler SV, Moorman DE, Smith RJ, James MH, Aston-Jones G (2014): Motivational activation: A unifying hypothesis of orexin/hypocretin function. Nat Neurosci 17:1298–1303.
2. Sakurai T, Amemiya A, Ishii M, Matsuzaki I, Chemelli RM, Tanaka H, *et al.* (1998): Orexins and orexin receptors: A family of hypothalamic neuropeptides and G protein-coupled receptors that regulate feeding behavior. Cell 92:573–585.
3. Scammell TE, Winrow CJ (2011): Orexin receptors: Pharmacology and therapeutic opportunities. Annu Rev Pharmacol Toxicol 51:243–266.
4. Li SB, Damonte VM, Chen C, Wang GX, Kebschull JM, Yamaguchi H, *et al.* (2022): Hyperexcitable arousal circuits drive sleep instability during aging. Science 375:eabh3021.
5. Lee MG, Hassani OK, Jones BE (2005): Discharge of identified orexin/hypocretin neurons across the sleep-waking cycle. J Neurosci 25:6716–6720.
6. Mochizuki T, Crocker A, McCormack S, Yanagisawa M, Sakurai T, Scammell TE (2004): Behavioral state instability in orexin knock-out mice. J Neurosci 24:6291–6300.
7. Vassalli A, Franken P (2017): Hypocretin (orexin) is critical in sustaining theta/gamma-rich waking behaviors that drive sleep need. Proc Natl Acad Sci U S A 114:E5464–E5473.
8. Liblau RS, Vassalli A, Seifinejad A, Tafti M (2015): Hypocretin (orexin) biology and the pathophysiology of narcolepsy with cataplexy. Lancet Neurol 14:318–328.
9. Jacobson LH, Hoyer D, de Lecea L (2022): Hypocretins (orexins): The ultimate translational neuropeptides. J Intern Med 291:533–556.
10. Johnson PL, Truitt W, Fitz SD, Minick PE, Dietrich A, Sanghani S, *et al.* (2010): A key role for orexin in panic anxiety. Nat Med 16:111–115.
11. Peleg-Raibstein D, Burdakov D (2021): Do orexin/hypocretin neurons signal stress or reward? Peptides 145:170629.
12. Eban-Rothschild A, Appelbaum L, de Lecea L (2018): Neuronal mechanisms for sleep/wake regulation and modulatory drive. Neuropsychopharmacology 43:937–952.
13. Villano I, Messina A, Valenzano A, Moscatelli F, Esposito T, Monda V, *et al.* (2017): Basal forebrain cholinergic system and orexin neurons: Effects on attention. Front Behav Neurosci 11:10.
14. Peyron C, Tighe DK, van den Pol AN, de Lecea L, Heller HC, Sutcliffe JG, Kilduff TS (1998): Neurons containing hypocretin (orexin) project to multiple neuronal systems. J Neurosci 18:9996–10015.
15. Seifinejad A, Vassalli A, Tafti M (2021): Neurobiology of cataplexy. Sleep Med Rev 60:101546.
16. Burgess CR, Scammell TE (2012): Narcolepsy: Neural mechanisms of sleepiness and cataplexy. J Neurosci 32:12305–12311.

17. Okura M, Fujiki N, Kita I, Honda K, Yoshida Y, Mignot E, Nishino S (2004): The roles of midbrain and diencephalic dopamine cell groups in the regulation of cataplexy in narcoleptic Dobermans. Neurobiol Dis 16:274–282.
18. Bandarabadi M, Li S, Aeschlimann L, Colombo G, Tzanoulinou S, Tafti M, *et al.* (2023): Inactivation of hypocretin receptor-2 signaling in dopaminergic neurons induces hyperarousal and enhanced cognition but impaired inhibitory control. Mol Psychiatry 29:327–341.
19. Mohammadkhani A, Mitchell C, James MH, Borgland SL, Dayas CV (2024): Contribution of hypothalamic orexin (hypocretin) circuits to pathologies of motivation. Br J Pharmacol 181:4430–4449.
20. Calipari ES, España RA (2012): Hypocretin/orexin regulation of dopamine signaling: Implications for reward and reinforcement mechanisms. Front Behav Neurosci 6:54.
21. James MH, Aston-Jones G (2022): Orexin reserve: A mechanistic framework for the role of orexins (hypocretins) in addiction. Biol Psychiatry 92:836–844.
22. Aston-Jones G, Smith RJ, Moorman DE, Richardson KA (2009): Role of lateral hypothalamic orexin neurons in reward processing and addiction. Neuropharmacology 56(suppl 1):112–121.
23. Brodnik ZD, Alonso IP, Xu W, Zhang Y, Kortagere S, España RA (2020): Hypocretin receptor 1 involvement in cocaine-associated behavior: Therapeutic potential and novel mechanistic insights. Brain Res 1731:145894.
24. Kalló I, Omrani A, Meye FJ, de Jong H, Liposits Z, Adan RAH (2022): Characterization of orexin input to dopamine neurons of the ventral tegmental area projecting to the medial prefrontal cortex and shell of nucleus accumbens. Brain Struct Funct 227:1083–1098.
25. Flagel SB, Clark JJ, Robinson TE, Mayo L, Czuj A, Willuhn I, *et al.* (2011): A selective role for dopamine in stimulus-reward learning. Nature 469:53–57.
26. Balcita-Pedicino JJ, Sesack SR (2007): Orexin axons in the rat ventral tegmental area synapse infrequently onto dopamine and gamma-aminobutyric acid neurons. J Comp Neurol 503:668–684.
27. Nakamura T, Uramura K, Nambu T, Yada T, Goto K, Yanagisawa M, Sakurai T (2000): Orexin-induced hyperlocomotion and stereotypy are mediated by the dopaminergic system. Brain Res 873:181–187.
28. Korotkova TM, Sergeeva OA, Eriksson KS, Haas HL, Brown RE (2003): Excitation of ventral tegmental area dopaminergic and nondopaminergic neurons by orexins/hypocretins. J Neurosci 23:7–11.
29. Borgland SL, Taha SA, Sarti F, Fields HL, Bonci A (2006): Orexin A in the VTA is critical for the induction of synaptic plasticity and behavioral sensitization to cocaine. Neuron 49:589–601.
30. Borgland SL, Storm E, Bonci A (2008): Orexin B/hypocretin 2 increases glutamatergic transmission to ventral tegmental area neurons. Eur J Neurosci 28:1545–1556.
31. Thomas CS, Mohammadkhani A, Rana M, Qiao M, Baimel C, Borgland SL (2022): Optogenetic stimulation of lateral hypothalamic orexin/dynorphin inputs in the ventral tegmental area potentiates mesolimbic dopamine neurotransmission and promotes reward-seeking behaviours. Neuropsychopharmacology 47:728–740.
32. Ford CP (2014): The role of D2-autoreceptors in regulating dopamine neuron activity and transmission. Neuroscience 282:13–22.
33. Baimel C, Lau BK, Qiao M, Borgland SL (2017): Projection-target-defined effects of orexin and dynorphin on VTA dopamine neurons. Cell Rep 18:1346–1355.
34. Fenwick EM, Marty A, Neher E (1982): A patch-clamp study of bovine chromaffin cells and of their sensitivity to acetylcholine. J Physiol 331:577–597.
35. Asahi S, Egashira SI, Matsuda M, Iwaasa H, Kanatani A, Ohkubo M, *et al.* (2003): Development of an orexin-2 receptor selective agonist, [Ala(11), D-Leu(15)]orexin-B. Bioorg Med Chem Lett 13:111–113.
36. Irukayama-Tomobe Y, Ogawa Y, Tominaga H, Ishikawa Y, Hosokawa N, Ambai S, *et al.* (2017): Nonpeptide orexin type-2 receptor agonist ameliorates narcolepsy-cataplexy symptoms in mouse models. Proc Natl Acad Sci USA 114:5731–5736.
37. Simon P, Dupuis R, Costentin J (1994): Thigmotaxis as an index of anxiety in mice. Influence of dopaminergic transmissions. Behav Brain Res 61:59–64.
38. File SE, Mabbutt PS, Hitchcott PK (1990): Characterisation of the phenomenon of "one-trial tolerance" to the anxiolytic effect of chlordiazepoxide in the elevated plus-maze. Psychopharmacology 102:98–101.
39. Treit D, Menard J, Royan C (1993): Anxiogenic stimuli in the elevated plus-maze. Pharmacol Biochem Behav 44:463–469.
40. Zhou H, Yu CL, Wang LP, Yang YX, Mao RR, Zhou QX, Xu L (2015): NMDA and D1 receptors are involved in one-trial tolerance to the anxiolytic-like effects of diazepam in the elevated plus maze test in rats. Pharmacol Biochem Behav 135:40–45.
41. Blomeley C, Garau C, Burdakov D (2017): Accumbal D2 cells orchestrate innate risk-avoidance according to orexin signals. Nat Neurosci 21:29–32.
42. Frussa-Filho R, Ribeiro A (2002): One-trial tolerance to the effects of chlordiazepoxide in the elevated plus-maze is not due to acquisition of a phobic avoidance of open arms during initial exposure. Life Sci 71:519–525.
43. File SE, Zangrossi H Jr, Viana M, Graeff FG (1993): Trial 2 in the elevated plus-maze: A different form of fear? Psychopharmacology 111:491–494.
44. Bari A, Dalley JW, Robbins TW (2008): The application of the 5-choice serial reaction time task for the assessment of visual attentional processes and impulse control in rats. Nat Protoc 3:759–767.
45. Razavi BM, Hosseinzadeh H (2017): A review of the role of orexin system in pain modulation. Biomed Pharmacother 90:187–193.
46. Bariselli S, Glangetas C, Tzanoulinou S, Bellone C (2016): Ventral tegmental area subcircuits process rewarding and aversive experiences. J Neurochem 139:1071–1080.
47. Solié C, Girard B, Righetti B, Tapparel M, Bellone C (2022): VTA dopamine neuron activity encodes social interaction and promotes reinforcement learning through social prediction error. Nat Neurosci 25:86–97.
48. Gunaydin LA, Deisseroth K (2014): Dopaminergic dynamics contributing to social behavior. Cold Spring Harb Symp Quant Biol 79:221–227.
49. Dawson M, Terstege DJ, Jamani N, Tsutsui M, Pavlov D, Bugescu R, *et al.* (2023): Hypocretin/orexin neurons encode social discrimination and exhibit a sex-dependent necessity for social interaction. Cell Rep 42:112815.
50. Abbas MG, Shoji H, Soya S, Hondo M, Miyakawa T, Sakurai T (2015): Comprehensive behavioral analysis of male Ox1r (-/-) mice showed implication of orexin Receptor-1 in mood, anxiety, and social behavior. Front Behav Neurosci 9:324.
51. Kim JG, Cron GO, Kim M, Hossain A, Lee JH (2026): Empathy and prosocial behavior powered by orexin-driven theta oscillations. Science 391:800–806.
52. McGraw M, Christensen C, Nelson H, Li AJ, Qualls-Creekmore E (2025): Divergent changes in social stress-induced motivation in male and female mice. Physiol Behav 291:114787.
53. Figueiredo Cerqueira MM, Castro MML, Vieira AA, Kurosawa JAA, Amaral Junior FLD, Siqueira Mendes FCC, Sosthenes MCK (2023): Comparative analysis between Open Field and Elevated Plus Maze tests as a method for evaluating anxiety-like behavior in mice. Heliyon 9:e14522.
54. Xiao X, Yeghiazaryan G, Cremer AL, Backes H, Kloppenburg P, Hausen AC (2023): Deficiency of orexin receptor type 1 in dopaminergic neurons increases novelty-induced locomotion and exploration. eLife 13:RP91716.
55. Bäckman CM, Malik N, Zhang Y, Shan L, Grinberg A, Hoffer BJ, *et al.* (2006): Characterization of a mouse strain expressing Cre recombinase from the 3′ untranslated region of the dopamine transporter locus. Genesis 44:383–390.
56. Li S, Franken P, Vassalli A (2018): Bidirectional and context-dependent changes in theta and gamma oscillatory brain activity in noradrenergic cell-specific hypocretin/orexin receptor 1-KO mice. Sci Rep 8:15474.

57. Ekstrand MI, Terzioglu M, Galter D, Zhu S, Hofstetter C, Lindqvist E, *et al.* (2007): Progressive parkinsonism in mice with respiratory-chain-deficient dopamine neurons. Proc Natl Acad Sci U S A 104:1325–1330.
58. Costa KM, Schenkel D, Roeper J (2021): Sex-dependent alterations in behavior, drug responses and dopamine transporter expression in heterozygous DAT-Cre mice. Sci Rep 11:3334.
59. Kroener S, Chandler LJ, Phillips PEM, Seamans JK (2009): Dopamine modulates persistent synaptic activity and enhances the signal-to-noise ratio in the prefrontal cortex. PLoS One 4:e6507.
60. Ott T, Nieder A (2019): Dopamine and cognitive control in prefrontal cortex. Trends Cogn Sci 23:213–234.
61. Stalter M, Westendorff S, Nieder A (2020): Dopamine gates visual signals in monkey prefrontal cortex neurons. Cell Rep 30:164–172.e4.
62. Salamone JD, Correa M (2024): The neurobiology of activational aspects of motivation: Exertion of effort, effort-based decision making, and the role of dopamine. Annu Rev Psychol 75:1–32.
63. Salinas-Hernández XI, Duvarci S (2021): Dopamine in fear extinction. Front Synaptic Neurosci 13:635879.
64. Salinas-Hernández XI, Zafiri D, Sigurdsson T, Duvarci S (2023): Functional architecture of dopamine neurons driving fear extinction learning. Neuron 111:3854–3870.e5.
65. Andolina D, Puglisi-Allegra S, Ventura R (2014): Strain-dependent differences in corticolimbic processing of aversive or rewarding stimuli. Front Syst Neurosci 8:207.
66. Freet CS, Arndt A, Grigson PS (2013): Compared with DBA/2J mice, C57BL/6J mice demonstrate greater preference for saccharin and less avoidance of a cocaine-paired saccharin cue. Behav Neurosci 127:474–484.
67. Zalocusky KA, Ramakrishnan C, Lerner TN, Davidson TJ, Knutson B, Deisseroth K (2016): Nucleus accumbens D2R cells signal prior outcomes and control risky decision-making. Nature 531:642–646.
68. Messore F, Narayanan Therpurakal R, Dufour J-P, Hoerder-Suabedissen A, Guidi L, Korrell K, *et al.* (2025): An orexin-sensitive subpopulation of layer 6 neurons regulates cortical excitability and anxiety behaviour. Transl Psychiatry 15:147.
69. Messore LF, Vadisiute A, Edmead H, Durmaz A, Abuelem M, Chedotal F, *et al.* (2025): Chronic silencing of Drd1a-Cre+ neurons impairs dopaminergic-driven cortical activation. Front Neuroanat 19: 1548545.
70. Wenger Combremont AL, Bayer L, Dupré A, Mühlethaler M, Serafin M (2016): Slow bursting neurons of mouse cortical Layer 6b are depolarized by hypocretin/orexin and major transmitters of arousal. Front Neurol 7:88.
71. Messore F, Narayanan Therpurakal R, Dufour JP, Hoerder-Suabedissen A, Guidi L, Korrell K, *et al.* (2025): An orexin-sensitive subpopulation of layer 6 neurons regulates cortical excitability and anxiety behaviour. Transl Psychiatry 15:147.
72. Zolnik TA, Bronec A, Ross A, Staab M, Sachdev RNS, Molnár Z, *et al.* (2024): Layer 6b controls brain state via apical dendrites and the higher-order thalamocortical system. Neuron 112:805–820.e4.
73. Langer SZ (1980): Presynaptic regulation of the release of catecholamines. Pharmacol Rev 32:337–362.
74. Wenger Combremont AL, Bayer L, Dupré A, Mühlethaler M, Serafin M (2016): Effects of hypocretin/orexin and major transmitters of arousal on fast spiking neurons in mouse cortical layer 6B. Cereb Cortex 26:3553–3562.
75. Crawley JN (2023): Twenty years of discoveries emerging from mouse models of autism. Neurosci Biobehav Rev 146:105053.
76. Crawley JN (2004): Designing mouse behavioral tasks relevant to autistic-like behaviors. Ment Retard Dev Disabil Res Rev 10:248–258.
77. Silverman JL, Thurm A, Ethridge SB, Soller MM, Petkova SP, Abel T, *et al.* (2022): Reconsidering animal models used to study autism spectrum disorder: Current state and optimizing future. Genes Brain Behav 21:e12803.
78. Genovese A, Butler MG (2023): The autism spectrum: Behavioral, psychiatric and genetic associations. Genes (Basel) 14:677.
79. Sato M, Nakai N, Fujima S, Choe KY, Takumi T (2023): Social circuits and their dysfunction in autism spectrum disorder. Mol Psychiatry 28:3194–3206.
80. Blouin AM, Fried I, Wilson CL, Staba RJ, Behnke EJ, Lam HA, *et al.* (2013): Human hypocretin and melanin-concentrating hormone levels are linked to emotion and social interaction. Nat Commun 4:1547.
81. Eriksson KS, Sergeeva O, Brown RE, Haas HL (2001): Orexin/hypocretin excites the histaminergic neurons of the tuberomammillary nucleus. J Neurosci 21:9273–9279.
82. Kukkonen JP, Turunen PM (2021): Cellular signaling mechanisms of hypocretin/orexin. Front Neurol Neurosci 45:91–102.
83. Muroya S, Funahashi H, Yamanaka A, Kohno D, Uramura K, Nambu T, *et al.* (2004): Orexins (hypocretins) directly interact with neuropeptide Y, POMC and glucose-responsive neurons to regulate Ca 2+ signaling in a reciprocal manner to leptin: Orexigenic neuronal pathways in the mediobasal hypothalamus. Eur J Neurosci 19:1524–1534.
84. Ma X, Zubcevic L, Brüning JC, Ashcroft FM, Burdakov D (2007): Electrical inhibition of identified anorexigenic POMC neurons by orexin/hypocretin. J Neurosci 27:1529–1533.
85. Belle MDC, Hughes ATL, Bechtold DA, Cunningham P, Pierucci M, Burdakov D, Piggins HD (2014): Acute suppressive and long-term phase modulation actions of orexin on the mammalian circadian clock. J Neurosci 34:3607–3621.
86. Izawa S, Fusca D, Jiang H, Heilinger C, Hausen AC, Wunderlich FT, *et al.* (2025): Orexin/hypocretin receptor 2 signaling in MCH neurons regulates REM sleep and insulin sensitivity. Cell Rep 44:115277.
87. Khaliq ZM, Bean BP (2010): Pacemaking in dopaminergic ventral tegmental area neurons: Depolarizing drive from background and voltage-dependent sodium conductances. J Neurosci 30:7401–7413.
88. Hatcher-Solis C, Fribourg M, Spyridaki K, Younkin J, Ellaithy A, Xiang G, *et al.* (2014): G protein-coupled receptor signaling to Kir channels in Xenopus oocytes. Curr Pharm Biotechnol 15:987–995.
89. Ishibashi M, Gumenchuk I, Miyazaki K, Inoue T, Ross WN, Leonard CS (2016): Hypocretin/orexin peptides alter spike encoding by serotonergic dorsal raphe neurons through two distinct mechanisms that increase the late afterhyperpolarization. J Neurosci 36:10097–10115.
90. Brodie MS, McElvain MA, Bunney EB, Appel SB (1999): Pharmacological reduction of small conductance calcium-activated potassium current (SK) potentiates the excitatory effect of ethanol on ventral tegmental area dopamine neurons. J Pharmacol Exp Ther 290:325–333.
91. Um KB, Kwak S, Cheon SH, Kim J, Hwang SK (2023): AST-001 improves social deficits and restores dopamine neuron activity in a mouse model of autism. Biomedicines 11:3283.
92. Stott JB, Greenwood IA (2024): G protein βγ regulation of KCNQ-encoded voltage-dependent K channels. Front Physiol 15: 1382904.
93. Morris LS, Costi S, Hameed S, Collins KA, Stern ER, Chowdhury A, *et al.* (2025): Effects of KCNQ potassium channel modulation on ventral tegmental area activity and connectivity in individuals with depression and anhedonia. Mol Psychiatry 30:3686–3694.
94. Chaki S (2025): Orexin receptors: Possible therapeutic targets for psychiatric disorders. Psychopharmacology 242:1669–1691.
95. Korotkova TM, Eriksson KS, Haas HL, Brown RE (2002): Selective excitation of GABAergic neurons in the substantia nigra of the rat by orexin/hypocretin in vitro. Regul Pept 104:83–89.
96. Liu C, Xue Y, Liu MF, Wang Y, Liu ZR, Diao HL, Chen L (2018): Orexins increase the firing activity of nigral dopaminergic neurons and participate in motor control in rats. J Neurochem 147:380–394.
97. Bian K, Liu C, Wang Y, Xue Y, Chen L (2021): Orexin-B exerts excitatory effects on nigral dopaminergic neurons and alleviates motor disorders in MPTP parkinsonian mice. Neurosci Lett 765:136291.
98. Léger L, Sapin E, Goutagny R, Peyron C, Salvert D, Fort P, Luppi PH (2010): Dopaminergic neurons expressing Fos during waking and paradoxical sleep in the rat. J Chem Neuroanat 39:262–271.
99. Cho JR, Treweek JB, Robinson JE, Xiao C, Bremner LR, Greenbaum A, Gradinaru V (2017): Dorsal raphe dopamine neurons modulate arousal and promote wakefulness by salient stimuli. Neuron 94:1205–1219.e8.

100. Korchynska S, Rebernik P, Pende M, Boi L, Alpár A, Tasan R, *et al.* (2022): A hypothalamic dopamine locus for psychostimulant-induced hyperlocomotion in mice. Nat Commun 13:5944.
101. Lu X, Xue J, Lai Y, Tang X (2024): Heterogeneity of mesencephalic dopaminergic neurons: From molecular classifications, electrophysiological properties to functional connectivity. FASEB J 38:e23465.
102. Ogawa Y, Kanda T, Vogt K, Yanagisawa M (2017): Anatomical and electrophysiological development of the hypothalamic orexin neurons from embryos to neonates. J Comp Neurol 525:3809–3820.
103. Grafe LA, Cornfeld A, Luz S, Valentino R, Bhatnagar S (2017): Orexins mediate sex differences in the stress response and in cognitive flexibility. Biol Psychiatry 81:683–692.
104. Grafe LA, Bhatnagar S (2020): The contribution of orexins to sex differences in the stress response. Brain Res 1731:145893.
105. Xiao X, Yeghiazaryan G, Eggersmann F, Cremer AL, Backes H, Kloppenburg P, Hausen AC (2025): Deficiency of orexin receptor type 1 in dopaminergic neurons increases novelty-induced locomotion and exploration. eLife 12:RP91716.
106. Summers CH, Yaeger JDW, Staton CD, Arendt DH, Summers TR (2020): Orexin/hypocretin receptor modulation of anxiolytic and antidepressive responses during social stress and decision-making: Potential for therapy. Brain Res 1731:146085.
107. McGregor R, Wu MF, Thannickal TC, Li S, Siegel JM (2024): Opioid-induced neuroanatomical, microglial and behavioral changes are blocked by suvorexant without diminishing opioid analgesia. Nat Ment Health 2:1018–1031.
108. Bonifazi A, Del Bello F, Giorgioni G, Piergentili A, Saab E, Botticelli L, *et al.* (2023): Targeting orexin receptors: Recent advances in the development of subtype selective or dual ligands for the treatment of neuropsychiatric disorders. Med Res Rev 43:1607–1667.
109. Zhuang C, Cao Y, Lu J, Zhou Y, Liu Y, Li Y (2025): The orexin/hypocretin system in dementia-related neurological disorders: A double-edged sword in cognitive impairment. Psychopharmacology 242:2161–2179.
110. Williams JT, Bolli MH, Brotschi C, Sifferlen T, Steiner MA, Treiber A, *et al.* (2024): Discovery of Nivasorexant (ACT-539313): The first selective Orexin-1 receptor antagonist (SO1RA) investigated in clinical trials. J Med Chem 67:2337–2348.
111. Reid MS, Tafti M, Nishino S, Sampathkumaran R, Siegel JM, Mignot E (1996): Local administration of dopaminergic drugs into the ventral tegmental area modulates cataplexy in the narcoleptic canine. Brain Res 733:83–100.
112. Dauvilliers Y, Mignot E, Del Río Villegas R, Du Y, Hanson E, Inoue Y, *et al.* (2023): Oral orexin receptor 2 agonist in narcolepsy Type 1. N Engl J Med 389:309–321.
113. Dauvilliers Y, Plazzi G, Mignot E, Lammers GJ, Del Río Villegas R, Khatami R, *et al.* (2025): Oveporexton, an oral orexin receptor 2-selective agonist, in narcolepsy Type 1. N Engl J Med 392:1905–1916.
114. Markovic T, Pedersen CE, Massaly N, Vachez YM, Ruyle B, Murphy CA, *et al.* (2021): Pain induces adaptations in ventral tegmental area dopamine neurons to drive anhedonia-like behavior. Nat Neurosci 24:1601–1613.